Computer Communications 196 (2022) 167–183

Contents lists available at ScienceDirect

Computer Communications

journal homepage: www.elsevier.com/locate/comcom

Decision fusion for multi-route and multi-hop Wireless Sensor Networks over the Binary Symmetric Channel

Gaoyuan Zhang [a,b,c], Kai Chen [a], Congfang Ma [a], Sravan Kumar Reddy [d], Baofeng Ji [a,c], Yongen Li [a], Congzheng Han [b], Xiaohui Zhang [a], Zhumu Fu [a,*]

[a] School of Information Engineering, Henan University of Science and Technology, Luoyang 471023, China
[b] Key Laboratory of Middle Atmosphere and Global Environment Observation, Institute of Atmospheric Physics, Chinese Academy of Sciences, Beijing 100029, China
[c] Science and Technology Innovation Center of Intelligent system, Longmen Laboratory, Luoyang 471023, China
[d] RGM college of Engineering and Technology, India

ARTICLE INFO

Keywords:
Decision fusion
Multi-route and multi-hop
Binary Symmetric Channel
Channel State Information

ABSTRACT

The decision fusion for multi-route and multi-hop Wireless Sensor Networks (WSNs) is studied, wherein a discrete memoryless channel model, i.e., the Binary Symmetric Channel (BSC), is considered to characterize the relay transmission of each hop from the local sensor to the fusion center. In particular, we first develop the optimal log-likelihood ratio (LLR) based decision fusion rule, wherein the fusion center is assumed to have perfect knowledge of both the local sensor performance indices and the Channel State Information (CSI), i.e., crossover probability for each BSC. Secondly, we derive the suboptimum and robust fusion rules for two cases. In the first case, channel condition from the source to the local sensor is considered to be ideal. In the second case, the crossover probability for each BSC is assumed to be relatively large or small. Our result show that our suboptimum fusion detectors require less or no a priori information about crossover probability and/or the local sensor performance indices, and thus are easy to implement. We also show that the simple decision fusion statistic, i.e., the counting-based statistic, can be directly derived from the optimal LLR-based statistic for both cases. These suboptimum fusion rules are clearly desired for applications, wherein perfect estimation of the local sensor performance and CSI is complexity-intensive or unachievable. Furthermore, the optimal LLR-based scheme for joint decision fusion and CSI estimation is proposed. We uniformly quantize the equivalent crossover probability into discrete status, and thus give a suboptimum but more computationally practical scheme. The performance evaluation is finally developed both analytically and through simulation.

1. Introduction

Much concentrations have been recently achieved on wireless sensor networks (WSNs) especially because of its appropriate application in "edge access" of future "Internet of Things (IoT)". In WSNs, a collection of sensor nodes are randomly distributed in a geographical area, and the sensing and measuring tasks are usually performed. Its typical applications include health care, environmental and structural monitoring, disaster recovery and rescue operations [1–4].

In such distributed networks, the fusion center (FC) gathers the decisions from the local sensors, and the global decision is then declared by the FC using a particular fusion rule [5]. Obviously, selecting reliable fusion rules is the key to obtain excellent detection performance. For some resource constrained wireless sensor networks, low complexity decision fusion schemes can save a lot of resources, which will greatly improve the work efficiency of the whole WSNs. Therefore, it is very important for academics to study the fusion rules used by fusion centers in Wireless Sensor Networks. To the best of our knowledge, several decision fusion schemes have been proposed in recent years [6–9]. The work of [6] pays attention towards distributed detection for multi-sensor millimeter wave (mmWave) massive multiple-input multiple-output (MIMO) WSNs, and low complexity fusion rules following the idea of hybrid combining are constructed. Local sensor decision rules based on an energy detector is introduced in [7], and the performance characteristics is also given. By ordering sensor transmissions, an energy-efficient counting rule for distributed detection is proposed in [8], wherein the sensors transmit their unquantized statistics to the fusion center in a sequential manner. Interestingly, in [9], the behavior of the max-product algorithm is analyzed in a distributed detection scenario. In fact, this algorithm can be considered as linear data-fusion as indicated in [9]. For a detailed discussion and an extensive list of references of decision fusion, the authors suggest [4].

* Corresponding author at: School of Information Engineering, Henan University of Science and Technology, Luoyang 471023, China.
E-mail address: fuzhumu@haust.edu.cn (Z. Fu).

https://doi.org/10.1016/j.comcom.2022.09.025
Received 29 June 2022; Received in revised form 20 August 2022; Accepted 28 September 2022
Available online 3 October 2022

Unlike those who were researching ways to develop decision fusion under single-hop WSNs, substantial work has also been devoted to optimizing the fusion process over multi-hop WSNs [10–15]. Note that, multi-hop transmission is of value for some resource-constrained WSNs. In this context, the multi-hop transmission is needed to relay the binary decisions from local sensors to reach a fusion center for minimal energy consumption.

The channel-aware likelihood ratio (LLR) based decision fusion for multi-hop relay WSNs over a fading environment is analyzed in [10]. However, the channel fading statistics are assumed to be known for the fusion center. In a heterogeneous WSN (HWSN), an iterative decision fusion algorithm is studied in [11], wherein the multi-hop transmission is needed to relay the sensed information from N heterogeneous access points to M heterogeneous FCs. In [12], to maximize the network lifetime and improve the surveillance coverage, a data collection mechanism is proposed for the HWSN, which uses a mobile sink to collect data. Distributed detection of sparse signals with censoring sensors in clustered multi-hop sensor networks is presented in [13]. By taking parameters of energy consumption balance, environmental metrics and reliability into consideration, [14] introduces a fusion-based routing algorithm, which is environment-aware as well as reliable. Interestingly, in [15], the minimum cuts detection problem is studied in a given wireless multi-hop network.

Unlike previous studies that too much emphasis on continuous channel, in this paper, the channel condition from the local sensor to the fusion center is considered to be Binary Symmetric Channel (BSC) [16]. Our main contributions are summarized as follows.

- We develop the optimal LLR-based decision fusion rule for multi-route and multi-hop WSNs over the BSC. The explicit and exact solution for the optimum statistic shows that perfect knowledge of the local sensor performance indices and the Channel State Information (CSI), i.e., crossover probability for each hop, should be prior completely known at the fusion center. Furthermore, the logarithm operation is also involved. These two intrinsic characteristics depict that the successfully implementation of the optimal scheme at the fusion center is complexity-intensive, and will consume high computation power especially when the number of route and relay node is large.
- We assume that the channel condition from the source to the local sensor is ideal, i.e., the local sensor performance is perfect. Then, we first show that the optimal fusion rule can be reduced to the suboptimum Chair–Varshney rule. Further, when the crossover probability for each relay BSC is relatively large, the optimal fusion rule further reduces to form reminiscent of a maximum ratio combining (MRC) statistic for fading mitigation in wireless communications with channel diversity. We also show that the simple decision fusion statistic, i.e., the counting-based decision fusion statistic, can also be adopted if the idea of equal gain combining (EGC) is directly borrowed. The statistic in the form of an selective combining (SC) is also given, wherein we select the local observation from the optimal relay channel. These suboptimum schemes are of various degrees of complexity.
- We also derive the robust suboptimum LLR-based fusion rules when the crossover probability for each relay BSC is relatively small or large. For the former case, we achieve a Chair–Varshney rule, and only a priori information about the local sensor performance indices is required. For the latter case, we develop a suboptimum fusion statistic with a analogs form of the MRC, wherein we further assume that the performance indices is invariable for each local sensor. The counting-based decision fusion statistic can also be surprisingly adopted in this case. That is, the fusion center does not need to take the prior information such as crossover probability and local sensor performance indices as the fusion conditions, which is feasible. This is clearly desired for applications, whenin perfect estimation of the local sensor performance indices and CSI is complexity-intensive or unachievable.
- The optimal LLR-based scheme for joint decision fusion and CSI estimation is also proposed. Our explicit and exact solution for this optimal joint decision fusion and CSI estimation shows that the search should be developed for each value in crossover probability space. This is clearly of high implementation complexity. Thus, we uniformly quantize the continuous crossover probability space into discrete status, and thus give a suboptimum but more computationally practical scheme. CSI estimation is absolutely necessary for decision fusion if channel coding is considered in the local sensor.
- The explicit and exact solution for performance analysis of a special case of counting-based decision fusion, i.e., majority-based decision fusion, is developed, wherein we assume that the local sensor performance indices and CSI is invariable for each transmission link. The extension to a special case, wherein the channel condition from the source to the local sensor is ideal, is also studied. Extensive simulations are finally designed and implemented to verify all of our fusion rules and performance analysis.

Please note that we concentrate on information fusion under coherent channels in the present work. However, if phase information is not known at the fusion center, the noncoherent fusion should be considered [17–24].

We organize the rest of this paper as follows. Section 2 focuses on the multi-hop parallel distributed transmission system over the BSC. The equivalent channel for multi-hop relay transmission is presented in Section 3. We develop the optimal LLR-based decision fusion in Section 4, while Section 5 concentrates on derivation of the suboptimum LLR-based decision fusion. The LLR-based scheme for joint decision fusion and CSI estimation is given in Section 6. The performance analysis is developed in Section 7. The simulation results are presented and discussed in Section 8. Finally, some conclusions and future work are provided in Section 9.

2. System model

Consider a parallel distributed decision fusion structure as depicted in Fig. 1, where the transmission of x_i from each local sensor to the fusion center is characterized by a multi-hop BSC model. Here, I independent sensors make local decisions with maximum-likelihood (ML) principle, and the data is generated according to two hypotheses under test, i.e., H_0 or H_1. Then these decisions are transmitted over J BSC channels in typical serial concatenation form to a fusion center, and the received data is denoted as y_i. Note that, the detection probability P_{di} and the false alarm probability P_{fi} is preferred to characterize the data transmission quality from the source to local sensors in the presence of channel error. We can use a variety of estimation methods to obtain them, such as the method based on the maximum likelihood ratio criterion proposed in [25]. In this paper, we assume that P_{di} and P_{fi} are completely known.

Here, without loss of generality and also for analysis convenience, we consider the BSC for data transmission from local sensors to the fusion center. A series of BSC channels may be equivalent to the total BSC channel in the transmission link. This makes the whole transmission process clearer, which will be discussed in Section 3. The extension to other channel case is straightforward but not pursued here. Furthermore, for simplicity in describing decision fusion principle, the relay node just forwards the impaired channel observation until it reaches the FC. Equivalently, the amplify and forward (AF) protocol is implemented at the relay node, for which however the amplification factor is set to be 1. This mainly takes into the consideration that energy as well as processing capabilities is limited for the relay node. However, the extension to other relay processing schemes, e.g., decode-and-forward (DF), is straightforward but also not pursued here.

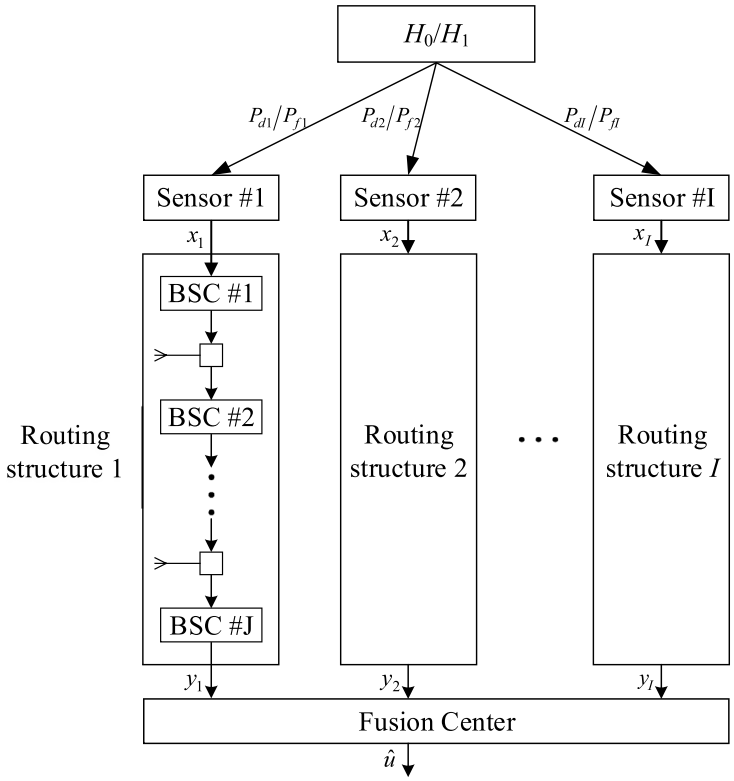

Fig. 1. Parallel distributed detection with multi-hop relay structure.

3. Equivalent channel for multi-hop relay transmission

Before launching the decision fusion discussion, two interesting lemmas will be given first. Let $\varepsilon_{i,j}$ be the crossover probability of the jth relay BSC in the ith routing, and the following can be derived.

Lemma 1. *The whole transmission from the local sensor to the FC can be equivalent to a BSC as shown in Fig. 2, which is obtained by cascading J BSC channels in series, and the crossover probability matrix is*

$$\begin{aligned}\begin{bmatrix} 1-\varepsilon_i & \varepsilon_i \\ \varepsilon_i & 1-\varepsilon_i \end{bmatrix} &= \begin{bmatrix} P\left(y_i=0\,|x_i=0\right) & P\left(y_i=1\,|x_i=0\right) \\ P\left(y_i=0\,|x_i=1\right) & P\left(y_i=1\,|x_i=1\right) \end{bmatrix} \\ &= \begin{bmatrix} \frac{1}{2}\left[1+\prod_{j=1}^{J}\left(1-2\varepsilon_{i,j}\right)\right] & 1-\frac{1}{2}\left[1+\prod_{j=1}^{J}\left(1-2\varepsilon_{i,j}\right)\right] \\ 1-\frac{1}{2}\left[1+\prod_{j=1}^{J}\left(1-2\varepsilon_{i,j}\right)\right] & \frac{1}{2}\left[1+\prod_{j=1}^{J}\left(1-2\varepsilon_{i,j}\right)\right] \end{bmatrix}.\end{aligned} \tag{1}$$

Proof. For each route, the local observation y_i at the FC can be expressed as [26]:

$$y_i = x_i \oplus \sum_{j=1}^{J} \oplus e_{i,j}, 1 \le i \le I, 1 \le j \le J, \tag{2}$$

where $e_{i,j}$ is the error for the jth relay BSC in the ith routing. Following from (2), we have that

$$\varepsilon_i = P\left(y_i \ne x_i\right) = P\left(\sum_{j=1}^{J} \oplus e_{i,j} = 1\right) = 1 - P\left(\sum_{j=1}^{J} \oplus e_{i,j} = 0\right). \tag{3}$$

Since the probability that an odd number of bits in $\left\{e_{i,1}, e_{i,2}, \ldots, e_{i,J}\right\}$ are "1" is $1-\frac{1}{2}\left\{1+\prod_{j=1}^{J}\left(1-2\varepsilon_{i,j}\right)\right\}$ [27], thus (3) can be rewritten as

$$\varepsilon_i = 1 - \frac{1}{2}\left\{1+\prod_{j=1}^{J}\left[1-2\varepsilon_{i,j}\right]\right\}, \tag{4}$$

where $\varepsilon_{i,j} = P\left(e_{i,j}=1\right)$ denotes the crossover probability for the jth relay BSC in the ith routing.

Lemma 2. *The channel capacity of the equivalent BSC in Lemma 1 is*

$$C = 1 - H\left(1-\frac{1}{2}\left\{1+\prod_{j=1}^{J}\left[1-2\varepsilon_{i,j}\right]\right\}, \frac{1}{2}\left\{1+\prod_{j=1}^{J}\left[1-2\varepsilon_{i,j}\right]\right\}\right). \tag{5}$$

Proof. Following from Lemma 1, we have that the channel transition matrix is a symmetric matrix. The corresponding channel capacity is (5) [28].

Here, we only discuss the equivalent BSC model from the local sensor to the fusion center, although that there are different noise levels from the actual signal source to the local sensor. In Section 4, we will study the channel conditions according to the detection probability, false alarm probability and equivalent BSC to obtain the LLR-based decision fusion.

4. Optimal LLR-based decision fusion

Given the conditional independence assumption of local observations, the optimal LLR-based decision fusion statistic can be easily derived as

$$\begin{aligned}\Lambda &= \log\frac{P\left(H_1\,|\mathbf{y}\right)}{P\left(H_0\,|\mathbf{y}\right)} = \log\frac{\prod_i P\left(H_1\,|y_i\right)}{\prod_i P\left(H_0\,|y_i\right)} = \log\left\{\prod_i\left[\frac{P\left(H_1\,|y_i\right)}{P\left(H_0\,|y_i\right)}\right]\right\} \\ &= \sum_i \log\frac{P\left(H_1\,|y_i\right)}{P\left(H_0\,|y_i\right)} = \sum_i \Lambda\left(y_i\right).\end{aligned} \tag{6}$$

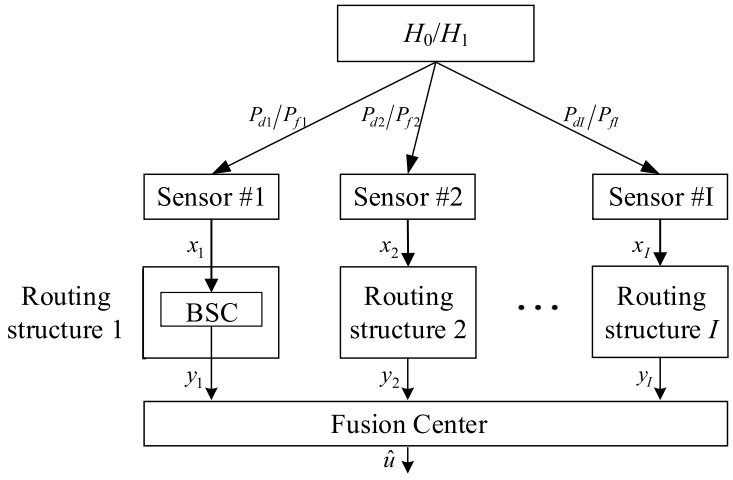

Fig. 2. Parallel distributed detection with equivalent relay channel structure.

Here, $\mathbf{y} = [y_1, y_2, \ldots, y_I]$ is a binary vector received at the fusion center, and it contains observations from all I local sensors after J hops. $\Lambda(y_i)$ can be considered as the optimal LLR-based decision statistic given the local observation y_i, which is critical to the final fusion detection. In the following, we will pay attention towards an explicit and exact solution for this metric.

Lemma 3. *The optimal LLR-based decision statistic, given the local observation y_i, can be given as*

$$\begin{aligned}\Lambda(y_i) &= \log \frac{P(H_1|y_i)}{P(H_0|y_i)} \\ &= \log \frac{P_{di}P(y_i|x_i=1) + (1-P_{di})P(y_i|x_i=0)}{P_{fi}P(y_i|x_i=1) + (1-P_{fi})P(y_i|x_i=0)}.\end{aligned} \tag{7}$$

Proof. See Appendix.

Following from Lemma 3, we have that when the local observation $y_i = 1$, $\Lambda(y_i)$ can be modified as

$$\Lambda(y_i) = \log \frac{P_{di}(1-\varepsilon_i) + (1-P_{di})\varepsilon_i}{P_{fi}(1-\varepsilon_i) + (1-P_{fi})\varepsilon_i}, \tag{8}$$

where ε_i is the crossover probability of the equivalent BSC obtained from serial concatenation of J BSC for the ith route as shown in Fig. 2. Note that, ε_i has been given in Lemma 1. Similarly, when $y_i = 0$, we may have that

$$\Lambda(y_i) = \log \frac{P_{di}\varepsilon_i + (1-P_{di})(1-\varepsilon_i)}{P_{fi}\varepsilon_i + (1-P_{fi})(1-\varepsilon_i)}. \tag{9}$$

Substituting (8) and (9) into (6), we get

$$\begin{aligned}\Lambda = &\sum_{i:y_i=1} \log \frac{P_{di}(1-\varepsilon_i) + (1-P_{di})\varepsilon_i}{P_{fi}(1-\varepsilon_i) + (1-P_{fi})\varepsilon_i} \\ &+ \sum_{i:y_i=0} \log \frac{P_{di}\varepsilon_i + (1-P_{di})(1-\varepsilon_i)}{P_{fi}\varepsilon_i + (1-P_{fi})(1-\varepsilon_i)}.\end{aligned} \tag{10}$$

Then, the final fusion criterion is

$$\hat{u} = \begin{cases} 1, & \text{if } \Lambda \geq \tau_1 \\ 0, & \text{if } \Lambda < \tau_1. \end{cases} \tag{11}$$

Here, τ_1 is the decision threshold.

The fusion detection process structure of the fusion center is shown in Fig. 3. In fact, after a simple analysis, we find that since the channel from the source to the local sensor is also a binary channel, and the transmission process from the source to the fusion center can be described equivalently by the configuration in Fig. 4. According to Fig. 4, it is easy to get the result given in (10).

As depicted in (10), the logarithmic operation is required, which introduces high complexity and consumes high computation power. Moreover, the fusion center should also have perfect knowledge of the CSI (i.e., crossover probability $\varepsilon_{i,j}$) and the local sensor performance indices (i.e., P_{di} and P_{fi}). Even if the fusion center can somehow estimate the CSI, it will be implementation-intensive. Furthermore, even if the local sensors can easily estimate their detection performances in real time, it will be very expensive to transmit them to the fusion center. In the following, we will pay attention towards suboptimum but more computationally practical decision fusion rules.

5. Suboptimum LLR-based decision fusion

5.1. Decision fusion for ideal local channel

We assume that the channel from the source to the local sensor is ideal, i.e., the channel condition is $P_{fi} = 0$, $P_{di} = 1$, and (10) can be expressed as

$$\begin{aligned}\Lambda &= \sum_{i:y_i=1} \log \frac{1-\varepsilon_i}{\varepsilon_i} + \sum_{i:y_i=0} \log \frac{\varepsilon_i}{1-\varepsilon_i} \\ &= \sum_i (-1)^{y_i} \log \frac{\varepsilon_i}{1-\varepsilon_i} = \sum_i \left[(2y_i - 1) \log \frac{1-\varepsilon_i}{\varepsilon_i}\right] \triangleq \Lambda_1.\end{aligned} \tag{12}$$

Clearly, Λ_1 resembles a MRC statistic for diversity combining, and the factor $\log \frac{1-\varepsilon_i}{\varepsilon_i}$ in (12) can be considered as the "fading gain" associated with the ith branch, which is determined by channel condition of all the hops as shown in (4). Let $\delta_{i,j} = \log \frac{1-\varepsilon_{i,j}}{\varepsilon_{i,j}}$, we know that the relationship between the $\tanh\theta$ and $\operatorname{arctanh}\theta$ is $2\operatorname{arctanh}\theta = \ln \frac{1+\tanh\theta}{1-\tanh\theta}$, then we can depict (12) as [29]:

$$\begin{aligned}\log \frac{1-\varepsilon_i}{\varepsilon_i} &= \log \frac{\frac{1}{2}\left[1 + \prod_{j=1}^{J}(1-2\varepsilon_{i,j})\right]}{1 - \frac{1}{2}\left[1 + \prod_{j=1}^{J}(1-2\varepsilon_{i,j})\right]} = \log \frac{1 + \prod_{j=1}^{J} \tanh\frac{\delta_{i,j}}{2}}{1 - \prod_{j=1}^{J} \tanh\frac{\delta_{i,j}}{2}} \\ &= 2\operatorname{arc}\tanh\left[\prod_{j=1}^{J} \tanh\frac{\delta_{i,j}}{2}\right] = \boldsymbol{\Phi}^{-1}\left\{\sum_{j=1}^{J} \boldsymbol{\Phi}\left[\delta_{i,j}\right]\right\}.\end{aligned} \tag{13}$$

In (13), we define that $\boldsymbol{\Phi}(x) = \boldsymbol{\Phi}^{-1}(x) = \ln \frac{e^x+1}{e^x-1} = -\ln\left(\tanh\frac{x}{2}\right)$. Note from the shape of $\boldsymbol{\Phi}(x)$ that the largest term in the sum of (13) corresponds to the smallest $\varepsilon_{i,j}$, so that, assuming that this term dominates the sum,

$$\boldsymbol{\Phi}^{-1}\left\{\sum_{j=1}^{J} \boldsymbol{\Phi}(\delta_{i,j})\right\} \approx \min_{1\leq j\leq J}\{\delta_{i,j}\}. \tag{14}$$

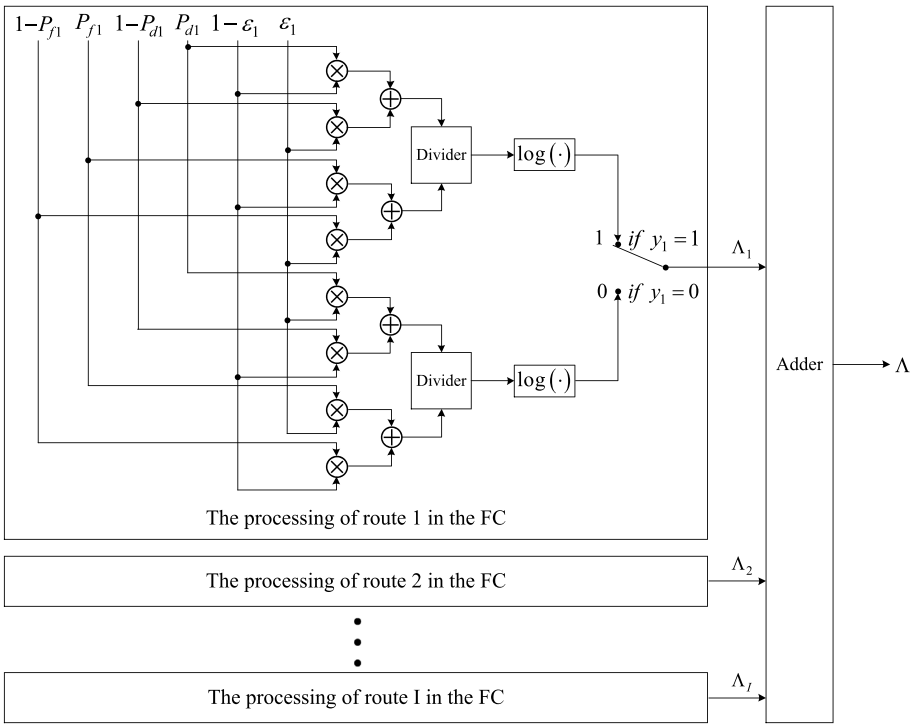

Fig. 3. Decision fusion process in fusion center.

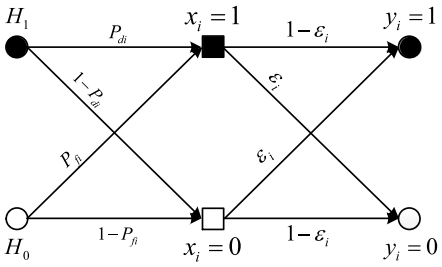

Fig. 4. Equivalent channel for transmission from binary source to fusion center.

According to the above derivation, another form of (12) can be derived as

$$\begin{aligned}\Lambda &= \sum_i \left[(2y_i - 1)\, \boldsymbol{\Phi}^{-1} \left\{ \sum_{j=1}^{J} \boldsymbol{\Phi}\left(\delta_{i,j}\right) \right\} \right] \\ &\approx \sum_i \left[(2y_i - 1) \min_{1\le j\le J} \left\{\delta_{i,j}\right\} \right] \triangleq \Lambda_2.\end{aligned} \tag{15}$$

As shown in (15), the "fading gain" now is only determined by the worst channel condition in all the hops. Finally, we propose a heuristic statistic in the simple form of an EGC that requires minimum amount of information:

$$\Lambda = \sum_i (2y_i - 1) \triangleq \Lambda_3. \tag{16}$$

In fact, when the quality of each equivalent transmission link is the same, (15) can be changed to

$$\Lambda = K_1 \sum_i (2y_i - 1), \tag{17}$$

where $K_1 = \log \frac{1-\varepsilon_i}{\varepsilon_i}$. The constant term K_1 is positive. Clearly, discarding K_1 will not affect the decision result, and (12) can also be transformed into (16).

Clearly, (16) can be termed as the counting-based fusion statistic, and no a priori information about crossover probability and the local sensor performance indices is needed at the fusion center. Note that, if the decision threshold τ_1 in (11) is set to be 0, we arrive at a special case of the counting-based fusion rule, i.e, majority-based fusion rule.

Motivated by above facts, we propose an alternative heuristic statistic from (12) in the form of an selective combining (SC) as follows:

$$\Lambda_4 \triangleq 2y_i - 1, \text{where } i = \arg\min \varepsilon_i. \tag{18}$$

5.2. Decision fusion for small crossover probability

When the crossover probability is small for each hop, i.e., $\varepsilon_i \to 0$, (8) can be modified as

$$\underset{\varepsilon_i \to 0}{\Lambda\left(y_i\right)} = \log \frac{P_{di}}{P_{fi}}. \tag{19}$$

Similarly, (9) can be given as

$$\underset{\varepsilon_i \to 0}{\Lambda\left(y_i\right)} = \log \frac{1-P_{di}}{1-P_{fi}}. \tag{20}$$

Substituting (19) and (20) into (10), we have that

$$\Lambda_5 \triangleq \sum_{i:\, y_i=1} \log \frac{P_{di}}{P_{fi}} + \sum_{i:\, y_i=0} \log \frac{1-P_{di}}{1-P_{fi}}. \tag{21}$$

As shown in (21), it does not require any knowledge of CSI but does require P_{di} and P_{fi} for all i. Correspondingly, significant performance loss is predicted for this approach especially for moderate or large crossover probability. We can term this as the Chair–Varshney fusion statistic [10]. Note that, for Chair–Varshney fusion, it assumes that the fusion center have reliable access to the local decision output.

5.3. Decision fusion for large crossover probability

We start by modifying the optimal LLR-based decision fusion statistic given in (8) as follows:

$$\begin{aligned}\Lambda\left(y_i\right) &= \log\frac{\left(1-P_{di}\right)+P_{di}\frac{1-\varepsilon_i}{\varepsilon_i}}{\left(1-P_{fi}\right)+P_{fi}\frac{1-\varepsilon_i}{\varepsilon_i}}\\ &= \log\frac{\left(1-P_{di}\right)+P_{di}\frac{\frac{1}{2}\left[1+\prod_{j=1}^{J}\left(1-2\varepsilon_{i,j}\right)\right]}{1-\frac{1}{2}\left[1+\prod_{j=1}^{J}\left(1-2\varepsilon_{i,j}\right)\right]}}{\left(1-P_{fi}\right)+P_{fi}\frac{\frac{1}{2}\left[1+\prod_{j=1}^{J}\left(1-2\varepsilon_{i,j}\right)\right]}{1-\frac{1}{2}\left[1+\prod_{j=1}^{J}\left(1-2\varepsilon_{i,j}\right)\right]}}\\ &= \log\frac{\left(1-P_{di}\right)+P_{di}\exp\left(\log\frac{\frac{1}{2}\left[1+\prod_{j=1}^{J}\left(1-2\varepsilon_{i,j}\right)\right]}{1-\frac{1}{2}\left[1+\prod_{j=1}^{J}\left(1-2\varepsilon_{i,j}\right)\right]}\right)}{\left(1-P_{fi}\right)+P_{fi}\exp\left(\log\frac{\frac{1}{2}\left[1+\prod_{j=1}^{J}\left(1-2\varepsilon_{i,j}\right)\right]}{1-\frac{1}{2}\left[1+\prod_{j=1}^{J}\left(1-2\varepsilon_{i,j}\right)\right]}\right)}\\ &= \log\frac{\left(1-P_{di}\right)+P_{di}\exp\left(2\operatorname{arc\,tanh}\left[\prod_{j=1}^{J}\tanh\frac{\delta_{i,j}}{2}\right]\right)}{\left(1-P_{fi}\right)+P_{fi}\exp\left(2\operatorname{arc\,tanh}\left[\prod_{j=1}^{J}\tanh\frac{\delta_{i,j}}{2}\right]\right)}\\ &= \log\frac{\left(1-P_{di}\right)+P_{di}\exp\left(\Phi^{-1}\left\{\sum_{j=1}^{J}\Phi\left[\delta_{i,j}\right]\right\}\right)}{\left(1-P_{fi}\right)+P_{fi}\exp\left(\Phi^{-1}\left\{\sum_{j=1}^{J}\Phi\left[\delta_{i,j}\right]\right\}\right)}\\ &\approx \log\frac{\left(1-P_{di}\right)+P_{di}\exp\left(\min_{1\le j\le J}\left\{\delta_{i,j}\right\}\right)}{\left(1-P_{fi}\right)+P_{fi}\exp\left(\min_{1\le j\le J}\left\{\delta_{i,j}\right\}\right)}.\end{aligned} \tag{22}$$

When the crossover probability for each hop is large, we have that $\varepsilon_{i,j}\to 0.5$, and $\delta_{i,j}\to 0$. Then, the exponential term in (22) can be approximated by using the first-order Taylor series expansion without undesired error. Therefore, (22) can be further simplified as

$$\begin{aligned}\Lambda\left(y_i\right) &\approx \log\frac{\left(1-P_{di}\right)+P_{di}\left(1+\min_{1\le j\le J}\left\{\delta_{i,j}\right\}\right)}{\left(1-P_{fi}\right)+P_{fi}\left(1+\min_{1\le j\le J}\left\{\delta_{i,j}\right\}\right)}\\ &= \log\frac{1+P_{di}\min_{1\le j\le J}\left\{\delta_{i,j}\right\}}{1+P_{fi}\min_{1\le j\le J}\left\{\delta_{i,j}\right\}}.\end{aligned} \tag{23}$$

Using the fact that, $x\to 0$, $\log(1+x)\approx x$, and the above statistic can be reduced to

$$\Lambda\left(y_i\right)\approx\left(P_{di}-P_{fi}\right)\min_{1\le j\le J}\left\{\delta_{i,j}\right\}. \tag{24}$$

Similarly, (9) can be simplified as

$$\begin{aligned}\Lambda\left(y_i(k)\right) &= \log\frac{P_{di}+\left(1-P_{di}\right)\frac{1-\varepsilon_i}{\varepsilon_i}}{P_{fi}+\left(1-P_{fi}\right)\frac{1-\varepsilon_i}{\varepsilon_i}}\\ &\approx \frac{P_{di}+\left(1-P_{di}\right)\left(1+\min_{1\le j\le J}\left\{\delta_{i,j}\right\}\right)}{P_{fi}+\left(1-P_{fi}\right)\left(1+\min_{1\le j\le J}\left\{\delta_{i,j}\right\}\right)}\\ &= \log\frac{1+\left(1-P_{di}\right)\min_{1\le j\le J}\left\{\delta_{i,j}\right\}}{1+\left(1-P_{fi}\right)\min_{1\le j\le J}\left\{\delta_{i,j}\right\}}\approx-\left(P_{di}-P_{fi}\right)\min_{1\le j\le J}\left\{\delta_{i,j}\right\}.\end{aligned} \tag{25}$$

Substituting (24) and (25) into (10), we have

$$\begin{aligned}\Lambda_6 &\triangleq \sum_i\Lambda\left(y_i\right)\\ &= \sum_{i:y_i=1}\left(P_{di}-P_{fi}\right)\min_{1\le j\le J}\left\{\delta_{i,j}\right\}-\sum_{i:y_i=0}\left(P_{di}-P_{fi}\right)\min_{1\le j\le J}\left\{\delta_{i,j}\right\}\\ &= \sum_i\left[\left(P_{di}-P_{fi}\right)\left(2y_i-1\right)\min_{1\le j\le J}\left\{\delta_{i,j}\right\}\right].\end{aligned} \tag{26}$$

Here, we also develop a statistic in a form of a MRC, which however the factor $\left(P_{di}-P_{fi}\right)\min_{1\le j\le J}\left\{\delta_{i,j}\right\}$ is now the "fading gain" associated with the ith branch.

Further, if the local sensors are identical, that is, P_{di} and P_{fi} do not change with i, and (26) can be given as

$$\begin{aligned}\Lambda_6 &= \left(P_d-P_f\right)\sum_i\left[\left\{2y_i-1\right\}\min_{1\le j\le J}\left\{\delta_{i,j}\right\}\right]\\ &= K_2\sum_i\left[\left(2y_i-1\right)\min_{1\le j\le J}\left\{\delta_{i,j}\right\}\right],\end{aligned} \tag{27}$$

where $K_2=\left(P_d-P_f\right)$. When $P_d-P_f>0$, discarding the constant term K_2 will not affect the decision result, and (27) becomes

$$\Lambda_6=\sum_i\min_{1\le j\le J}\left[\left(2y_i-1\right)\left\{\delta_{i,j}\right\}\right]. \tag{28}$$

Clearly, if we directly borrow the idea from EGC, we have that

$$\Lambda_7\triangleq\sum_i\left(2y_i-1\right). \tag{29}$$

6. Joint decision fusion and CSI estimation

6.1. Optimal joint decision fusion and CSI estimation

Considering that the cross probability ε_i of BSC obtained after the equivalence of multi-hop relay transmission process is modeled as a non random parameter, the basic principle of generalized likelihood ratio test (GLRT) is considered to realize joint detection fusion and CSI estimation. Here, we can have that

$$\left(\hat{u},\hat{\varepsilon}_i\right)=\arg\max_H\left\{\max_{\varepsilon_i}\prod_i P\left(H\left|y_i,\varepsilon_i\right.\right)\right\}. \tag{30}$$

According to the certification process in Appendix:

$$\prod_i P\left(H\left|y_i,\varepsilon_i\right.\right)\propto\prod_i\left\{\sum_{x_i}P\left(x_i\left|H\right.\right)P\left(y_i\left|x_i,\varepsilon_i\right.\right)\right\}, \tag{31}$$

where $\propto$ is used to indicate that the quantities are equal up to irrelevant quantities that do not affect the maximization. The fusion decision metric based on LLR can be obtained from (30) and (31):

$$\begin{aligned}\Lambda &= \log\frac{\prod_i P\left(H_1\left|y_i,\varepsilon_i\right.\right)}{\prod_i P\left(H_0\left|y_i,\varepsilon_i\right.\right)}=\log\frac{\prod_i\left\{\sum_{x_i}P\left(x_i\left|H_1\right.\right)P\left(y_i\left|x_i,\varepsilon_i\right.\right)\right\}}{\prod_i\left\{\sum_{x_i}P\left(x_i\left|H_0\right.\right)P\left(y_i\left|x_i,\varepsilon_i\right.\right)\right\}}\\ &= \sum_i\log\frac{\sum_{x_i}P\left(x_i\left|H_1\right.\right)P\left(y_i\left|x_i,\varepsilon_i\right.\right)}{\sum_{x_i}P\left(x_i\left|H_0\right.\right)P\left(y_i\left|x_i,\varepsilon_i\right.\right)}=\sum_i\Lambda\left(y_i,\varepsilon_i\right),\end{aligned} \tag{32}$$

where

$$\Lambda\left(y_i,\varepsilon_i\right)=\log\frac{\sum_{x_i}P\left(x_i\left|H_1\right.\right)P\left(y_i\left|x_i,\varepsilon_i\right.\right)}{\sum_{x_i}P\left(x_i\left|H_0\right.\right)P\left(y_i\left|x_i,\varepsilon_i\right.\right)}. \tag{33}$$

The final joint fusion and estimation criteria are

$$\hat{\varepsilon}_i=\arg\max_{\varepsilon_i}\left|\Lambda\right|, \tag{34}$$

$$\hat{u}=\begin{cases}1, & \text{if }\sum_i\Lambda\left(y_i,\hat{\varepsilon}_i\right)\ge\tau_2\\ 0, & \text{if }\sum_i\Lambda\left(y_i,\hat{\varepsilon}_i\right)<\tau_2.\end{cases} \tag{35}$$

Here, τ_2 is the decision threshold.

6.2. Practical joint decision fusion and CSI estimation

As can be seen from (34), the optimal joint detection and estimation scheme requires infinite dimensional search for the cross probability ε_i. This is clearly extremely complex. Note that, the fusion detection cannot be implemented in the second stage if the cross probability ε_i is not be successfully estimated in the first stage. Here, we quantize the continuous cross probability ε_i to reduce the implementation complexity of the optimal scheme. For convenience of implementation, the simplest uniform quantization is considered. In particular, when the number of the quantization intervals is denoted as m, we have

$$\varepsilon_i\in\left\{\frac{m}{2M},\quad m=1,2,\cdots,M\right\}. \tag{36}$$

7. Performance analysis

7.1. Performance analysis for majority-based decision fusion when the cross probability is large

The fusion detection error probability P_e can be expressed as

$$P_e = P\left(H_1\right) P\left(\hat{u}=0\left|H_1\right.\right) + P\left(H_0\right) P\left(\hat{u}=1\left|H_0\right.\right). \tag{37}$$

Let $K_0 = |S_0|$, where $S_0 = \{y_i : y_i = 0\}$, i.e., K_0 is the cardinality of S_0. Similarly, let $K_1 = |S_1|$, where $S_1 = \{y_i : y_i = 1\}$. With these definitions, for the majority-based decision fusion, we have that (37) can be modified as

$$P\left(\hat{u}=0\left|H_1\right.\right) = P\left(K_0 \geq I_\tau \left|H_1\right.\right) = P\left(K_1 < I_\tau \left|H_1\right.\right). \tag{38}$$

In the above formula, both K_0 and K_1 obey binomial distribution. I_τ is the threshold, and its value ranges from 0 to I. For majority-based decision fusion, we have that $I_\tau = I/2$. When H_1 is true, we can get

$$\begin{cases} K_0 \sim B\left(I, P_{01}\right) \\ K_1 \sim B\left(I, P_{11}\right), \end{cases} \tag{39}$$

where

$$\begin{cases} P_{01} = P\left(y_i=0|H_1\right) = P_{di}\varepsilon_i + \left(1-P_{di}\right)\left(1-\varepsilon_i\right) \\ P_{11} = P\left(y_i=1|H_1\right) = P_{di}\left(1-\varepsilon_i\right) + \left(1-P_{di}\right)\varepsilon_i. \end{cases} \tag{40}$$

Then (38) can be rewritten as

$$P\left(\hat{u}=0\left|H_1\right.\right) = \sum_{m=I_\tau}^{I} \binom{I}{m} P_{01}^m \left(1-P_{01}\right)^{I-m}. \tag{41}$$

According to Central limit theorem, when there are a large number of routes, we can get

$$P\left(\hat{u}=0\left|H_1\right.\right) \approx Q\left(\frac{I_\tau - IP_{01}}{\sqrt{IP_{01}\left(1-P_{01}\right)}}\right), \tag{42}$$

where Q function is complementary cumulative distribution function. Similarly, we have that

$$P\left(\hat{u}=1\left|H_0\right.\right) = P\left(K_1 \geq I_\tau \left|H_0\right.\right) = P\left(K_0 < I_\tau \left|H_0\right.\right). \tag{43}$$

When H_0 is true, we can get

$$\begin{cases} K_0 \sim B\left(I, P_{00}\right) \\ K_1 \sim B\left(I, P_{10}\right), \end{cases} \tag{44}$$

where

$$\begin{cases} P_{00} = P\left(y_i=0|H_0\right) = P_{fi}\varepsilon_i + \left(1-P_{fi}\right)\left(1-\varepsilon_i\right) \\ P_{10} = P\left(y_i=1|H_0\right) = P_{fi}\left(1-\varepsilon_i\right) + \left(1-P_{fi}\right)\varepsilon_i. \end{cases} \tag{45}$$

Then (43) can become

$$P\left(\hat{u}=1\left|H_0\right.\right) = \sum_{m=I_\tau}^{I} \binom{I}{m} P_{10}^m \left(1-P_{10}\right)^{I-m}. \tag{46}$$

When the number of route is extremely large, we have

$$P\left(\hat{u}=1\left|H_0\right.\right) \approx Q\left(\frac{I_\tau - IP_{10}}{\sqrt{IP_{10}\left(1-P_{10}\right)}}\right). \tag{47}$$

Substituting (46) and (47) into (37), we have

$$P_e \approx \frac{1}{2}Q\left(\frac{I_\tau - IP_{01}}{\sqrt{IP_{01}\left(1-P_{01}\right)}}\right) + \frac{1}{2}Q\left(\frac{I_\tau - IP_{10}}{\sqrt{IP_{10}\left(1-P_{10}\right)}}\right). \tag{48}$$

According to (48), it can be seen that the fusion detection error probability P_e is affected by such factors as the threshold I_τ, the number of routes I, P_{01} and P_{10}. Since $I_\tau = I/2$, (48) can be further written as

$$P_e \approx \frac{1}{2}Q\left(\frac{I/2 - IP_{01}}{\sqrt{IP_{01}\left(1-P_{01}\right)}}\right) + \frac{1}{2}Q\left(\frac{I/2 - IP_{10}}{\sqrt{IP_{10}\left(1-P_{10}\right)}}\right)$$

$$= \frac{1}{2}Q\left(\frac{I\left(1/2-P_{01}\right)}{\sqrt{I}\sqrt{1/4-\left(1/2-P_{01}\right)^2}}\right) + \frac{1}{2}Q\left(\frac{I\left(1/2-P_{10}\right)}{\sqrt{I}\sqrt{1/4-\left(1/2-P_{10}\right)^2}}\right) \tag{49}$$

$$= \frac{1}{2}Q\left(\frac{\sqrt{I}\left(1/2-P_{01}\right)}{\sqrt{1/4-\left(1/2-P_{01}\right)^2}}\right) + \frac{1}{2}Q\left(\frac{\sqrt{I}\left(1/2-P_{10}\right)}{\sqrt{1/4-\left(1/2-P_{10}\right)^2}}\right).$$

Let $t = \frac{\sqrt{I}\left(1/2-P_{01}\right)}{\sqrt{1/4-\left(1/2-P_{01}\right)^2}}$, and the following analysis results can be obtained.

We first assume that the number of routes I is set to be fixed. When $P_{01} \leq 1/2$, we can get $t \geq 0$. From the definition, we can see that with the increase of P_{01}, t is monotonically decreasing. According to the properties of Q function, we can get that P_e is monotonically increasing. If the number of routes I is increased, the fusion detection error probability will be reduced. Similarly, when $P_{01} > 1/2$, we can get $t < 0$. With the increase of P_{01}, t is monotonically decreasing. In combination with the properties of Q function, we can also obtain that P_e is monotonically increasing. However, if the number of routes is increased, the fusion detection error probability will also be increased.

Let us make a summary. First, the fusion detection error probability P_e increases monotonically with the increase of ε_i. Secondly, by improving the performance of local sensors, the detection performance will be improved. Finally, when P_{01} and P_{10} are less than or equal to 0.5, increasing the number of routes will also improve the performance. However, when P_{01} and P_{10} are greater than 0.5, increasing the number of routes will deteriorate the system performance.

7.2. Performance analysis for majority-based decision fusion under ideal local channel

When the channel from the source to the local sensor is ideal, we have that $P_{fi} = 0$ and $P_{di} = 1$. In this context, (40) and (45) can be respectively modified as

$$\begin{cases} P_{01} = P\left(y_i=0|H_1\right) = \varepsilon_i \\ P_{11} = P\left(y_i=1|H_1\right) = \left(1-\varepsilon_i\right), \end{cases} \tag{50}$$

and

$$\begin{cases} P_{00} = P\left(y_i=0|H_0\right) = \left(1-\varepsilon_i\right) \\ P_{10} = P\left(y_i=1|H_0\right) = \varepsilon_i. \end{cases} \tag{51}$$

With the above result, we have

$$P_e \approx Q\left(\frac{I_\tau - I\varepsilon_i}{\sqrt{I\varepsilon_i\left(1-\varepsilon_i\right)}}\right). \tag{52}$$

Similarly, according to (52), we have that the fusion detection error probability P_e monotonically increases with the increase of the cross probability. In particular, if the crossover probability ε_i is less than 0.5, increasing the number of routes will improve the detection performance. However, the detection performance will deteriorate by increasing the number of routes when the cross probability is greater than or equal to 0.5.

8. Numerical results and discussion

In this part, we analyze the fusion performance from many different aspects, including bit error rate (BER), frame error rate (FER), and complexity analysis. In the simulation, the crossover probability of the relay channel varies from 0.001 to 0.3. We also study the system performance of optimal LLR-based decision fusion and suboptimum LLR-based decision fusion under dynamic channel conditions. Then the joint decision fusion and CSI estimation are simulated, and the BER

Table 1
Parameters used in simulations.

Parameter	Detailed description
Channel condition	BSC
Channel parameters	Uniform reduction in interval (0.001, 0.3)
Information sequence length	504 bits
Noise condition	Obey Wiener distribution
Number of sensors	1, 3, 5, 7, 9, 30, 50, 100
Number of hops	1, 2, 3, 4, 5
Quantized quantity M	5
Full complexity LLR	(10)
Simplified LLR	(16), (21), (29)
Channel conditions of different paths	Obey the same crossover probability
Number of cycles	Get at least 3000 frame errors

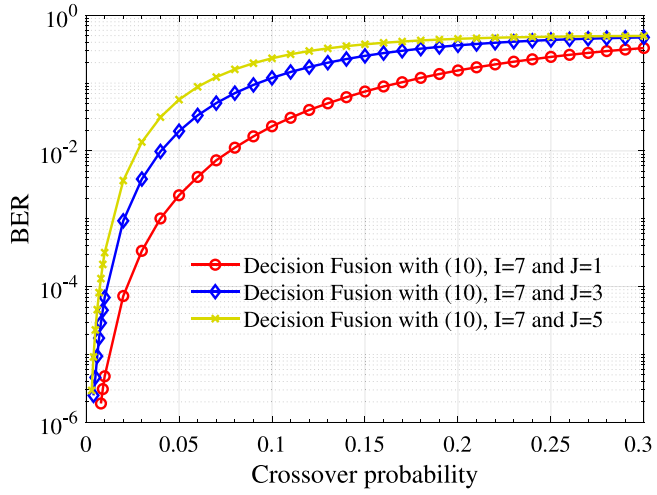

Fig. 5. BER performance of the optimal decision fusion. The number of route is set to be 7, and the relay number is 1, 3, and 5.

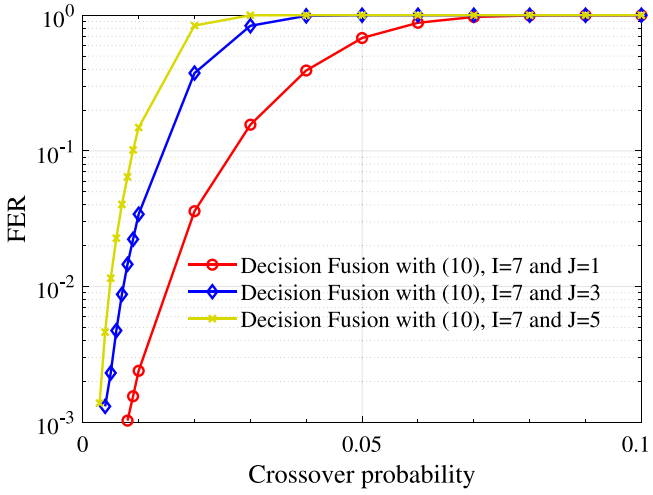

Fig. 6. FER performance of the optimal decision fusion. The number of route is set to be 7, and the relay number is 1, 3, and 5.

performance, FER performance and CSI estimation performance are discussed and analyzed.

We characterize the crossover probability for each hop as $\varepsilon_{i,j+1} = \varepsilon_{i,j} + \Delta_{i,j}$, where $\Delta_{i,j}$ is an independent Gaussian random variable with known variance $\sigma^2_{i,j}$ and mean 0. For initial crossover probability $\varepsilon_{i,1}$, the uniform distribution in 0.001 to 0.3 is considered. The length of each transmission data sequence is 504 bits. We collected at least 3000 frames of errors in each simulation process. Detailed simulation parameters are shown in Table 1.

8.1. Performance of the optimal decision fusion

Figs. 5 and 6 shows the impact of relay number on performance under the optimal LLR-based decision fusion, when the route number is set to be $I = 7$. As shown in Figs. 5 and 6, we can find that with the decrease of cross probability, the BER and FER performance show a threshold phenomenon. When the cross probability is greater than the threshold, the graph changes slowly and when the cross probability is less than the threshold, the BER and FER performance decrease rapidly with the decrease of error transfer probability, especially in FER performance. Under the same number of routes, the performance of the system begins to decline with the increase of hops, when the crossover probability is fixed to 0.008, the BER values of 1, 3 and 5 hops are 1.893×10^{-6}, 2.911×10^{-5} and 1.313×10^{-4} respectively.

At the same time, we studied the impact of route number, as shown in Figs. 7 and 8. We set the route number to be 1, 3, 5, 7 or 9 to explore the routing gain of the optimal LLR-based Decision Fusion. It is clearly observed that with the increase of the number of routes, the performance improves significantly. We take the crossover probability as 0.007, when there is only 1 route in the communication process, the

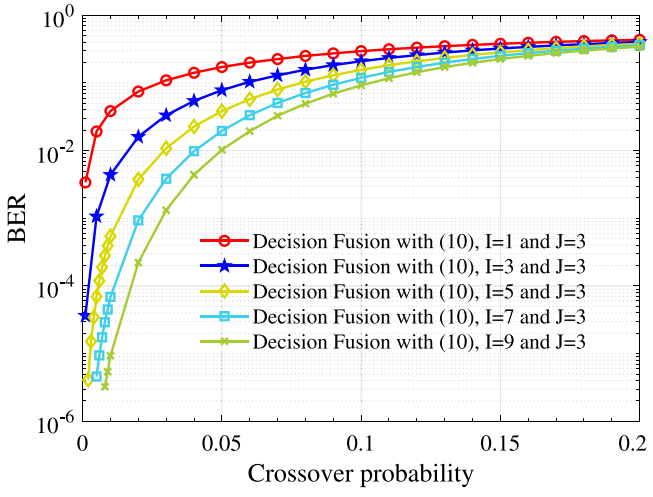

Fig. 7. BER performance of the optimal decision fusion. The number of route is set to be 1, 3, 5, 7, or 9, and the relay number is 3.

FER value of the system is 6.489×10^{-1}. However, when there are 9 routes, the FER value of the system is 8.348×10^{-4}.

In addition, we simulate the impact of noise variance on system performance. From Figs. 9 and 10, we can see that when the standard deviation of noise is below 0.01, there is no obvious fading. As the value increases, the channel condition of the system becomes very bad, so unavoidable performance degradation occurs.

Figs. 11 and 12 show the impact on system performance when the number of routes and relays changes simultaneously. We find that the

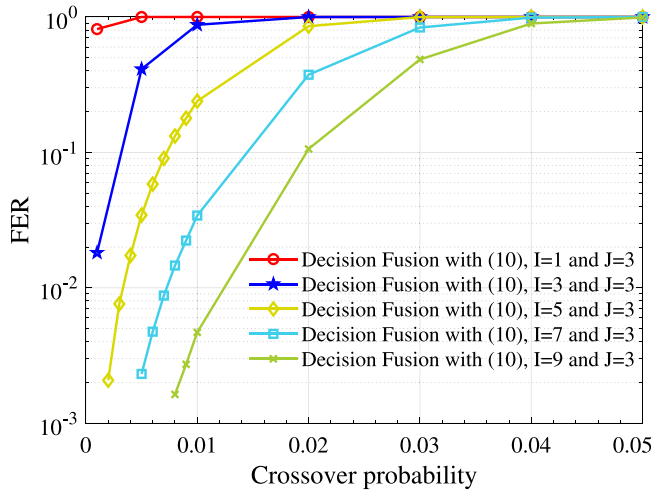

Fig. 8. FER performance of the optimal decision fusion. The number of route is set to be 1, 3, 5, 7, or 9, and the relay number is 3.

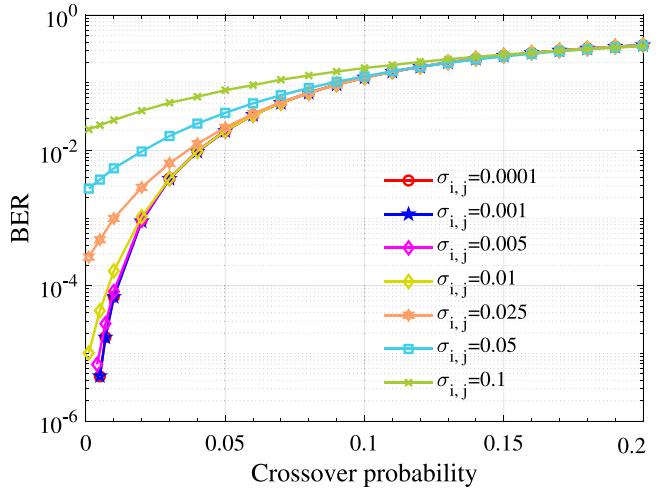

Fig. 9. BER performance for optimal decision fusion with (10). The route number is 7 and the relay number is 3.

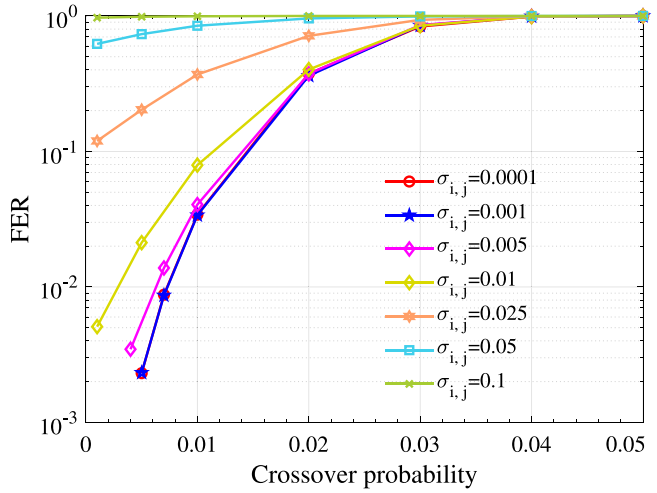

Fig. 10. FER performance of different noise variance under optimal decision fusion (10). the route number is 7 and the relay number is 3.

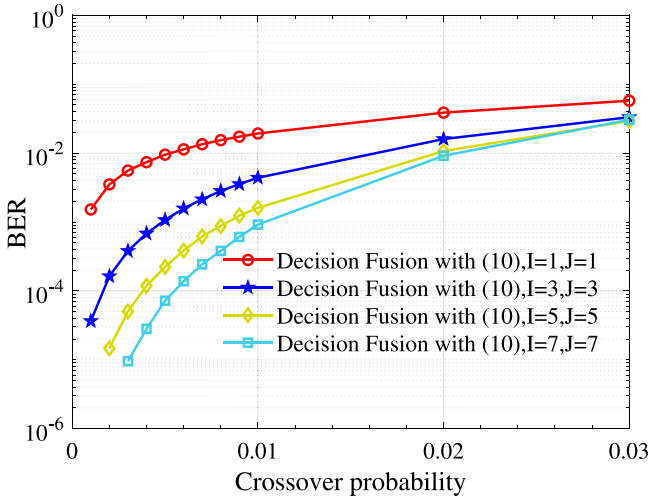

Fig. 11. BER performance for optimal decision fusion with (10). The route number is set to be 1, 3, 5, 7 and the relay number is set to be 1, 3, 5, 7.

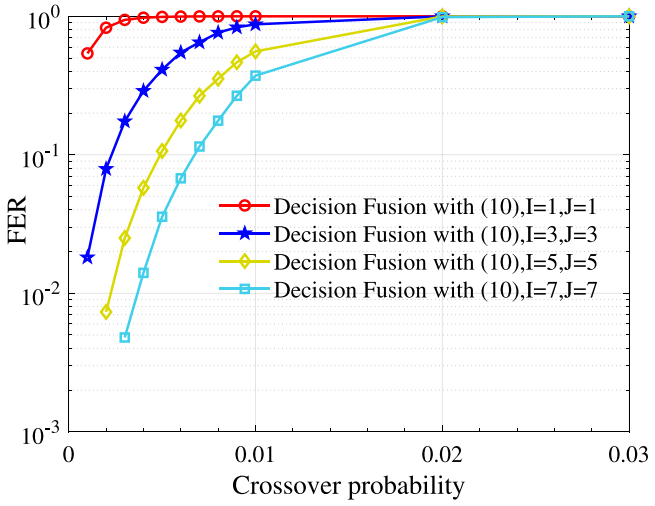

Fig. 12. FER performance for optimal decision fusion with (10). The route number is set to be 1, 3, 5, 7 and the relay number is set to be 1, 3, 5, 7.

BER and FER performance of the system is improved with the increase of the number of routes and relays. This also shows that the gain obtained by increasing the number of routes is higher than the fading caused by relays.

8.2. Performance when the local channel is ideal

When the channel from the source to the sensor is ideal, that is, $P_{fi} = 0$, $P_{di} = 1$. Firstly, we simulate the proposed decision fusion with (16) and compared it with its theoretical performance in Fig. 13. The number of routes is set to be 7 and the hops are 1, 3, 5. It is clear that the overall trend of the actual simulation curve and the theoretical curve is approximately the same, especially when the number of hops increases. According to (14), the smallest $\delta_{i,j}$ is usually obtained when the crossover probability $\varepsilon_{i,j}$ of the relay is the largest. Therefore, the coincidence between the performance simulation and the theoretical analysis may have deviation when the crossing probability is small.

Figs. 14 to 17 show the simulation results of the decision fusion with (12) , we can find that there is the same threshold phenomenon. Different from the previous information source is not ideal, the curve is smoother and not as steep as before, which also shows that the

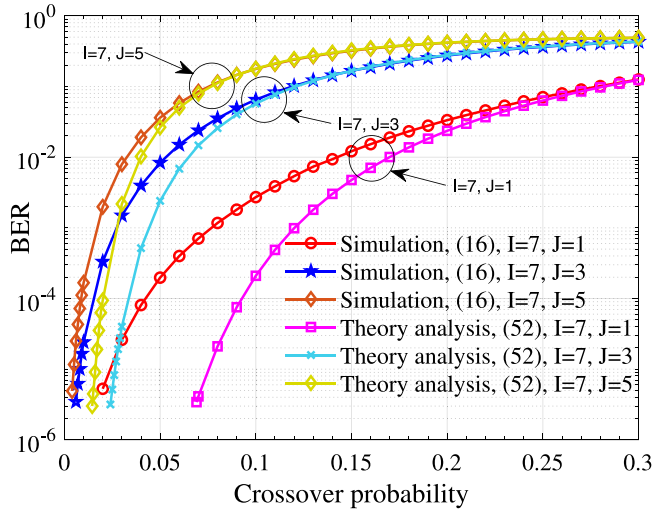

Fig. 13. Simulation result and theory analysis for majority-based fusion decision when the local channel is ideal.

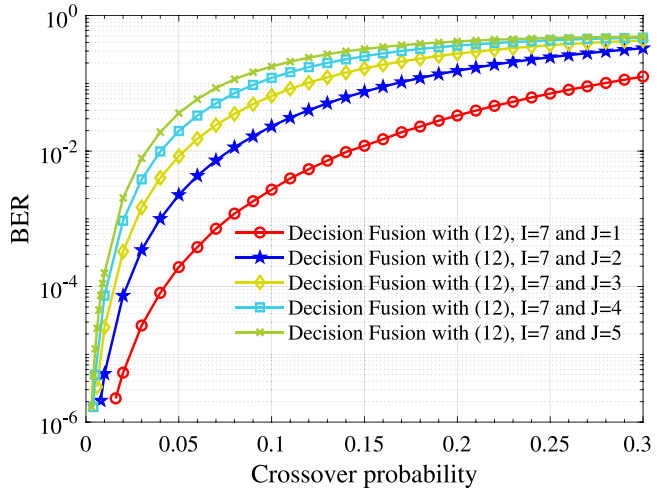

Fig. 14. BER performance of decision fusion with (12). The number of route is set to be 7, and the relay number varies from 1 to 5.

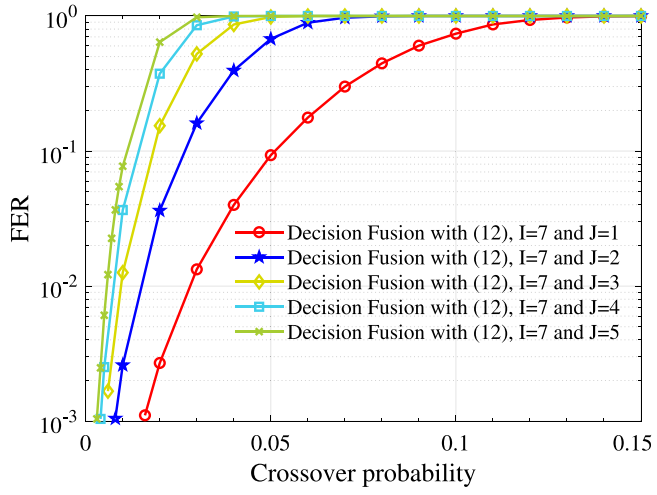

Fig. 15. FER performance of decision fusion with (12). The number of route is set to be 7, and the relay number varies from 1 to 5.

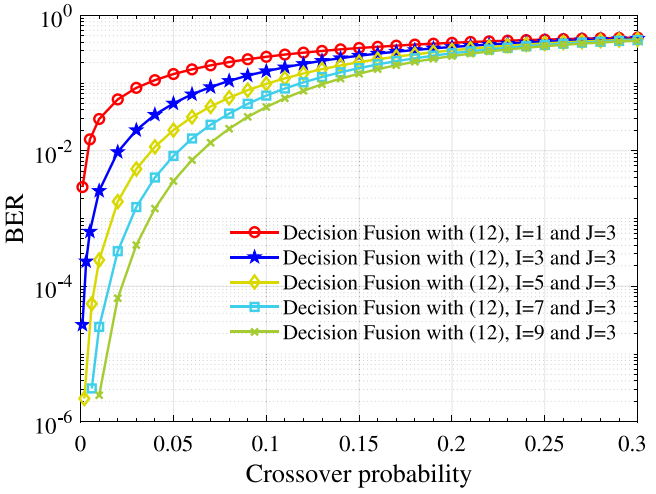

Fig. 16. BER performance of decision fusion with (12). The number of relay is set to be 3, and the route number varies from 1 to 9.

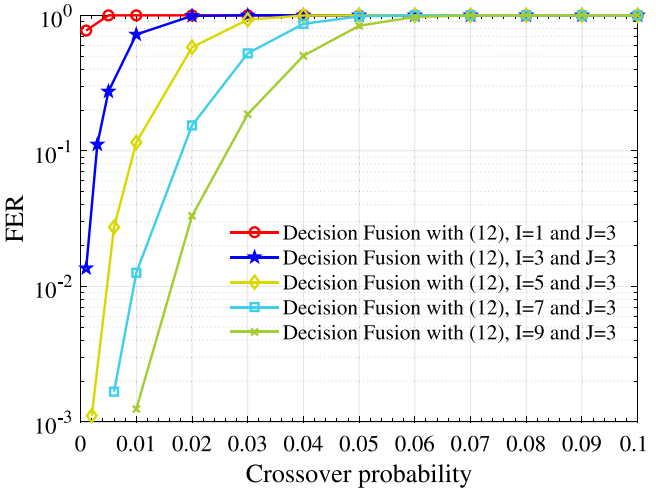

Fig. 17. FER performance of decision fusion with (12). The number of relay is set to be 3, and the route number varies from 1 to 9.

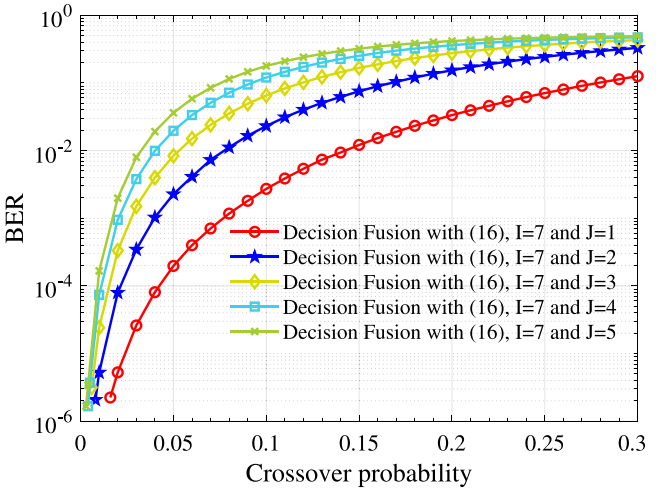

Fig. 18. BER performance of decision fusion with (16). The number of route is set to be 7, and the relay number varies from 1 to 5.

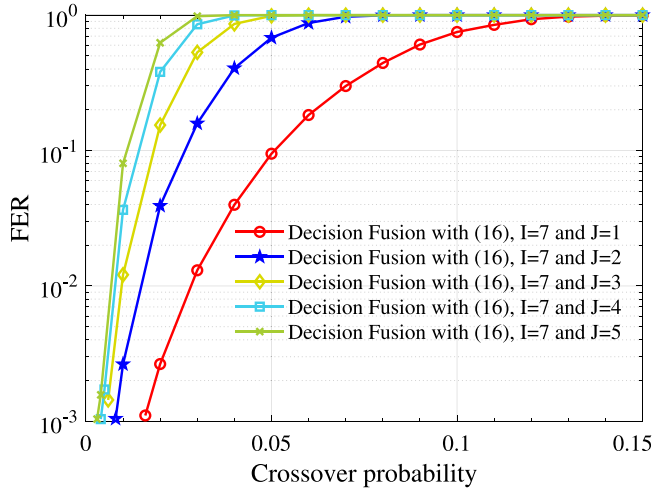

Fig. 19. FER performance of decision fusion with (16). The number of route is set to be 7, and the relay number varies from 1 to 5.

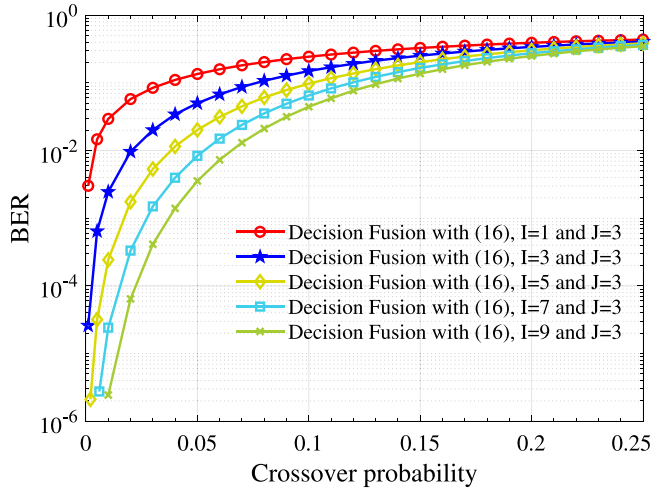

Fig. 20. BER performance of decision fusion with (16). The number of relay is set to be 3, and the route number varies from 1 to 9.

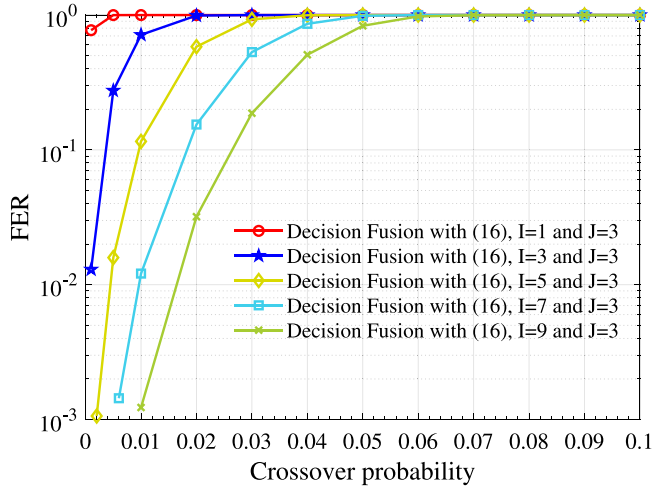

Fig. 21. FER performance of decision fusion with (16). The number of relay is set to be 3, and the route number varies from 1 to 9.

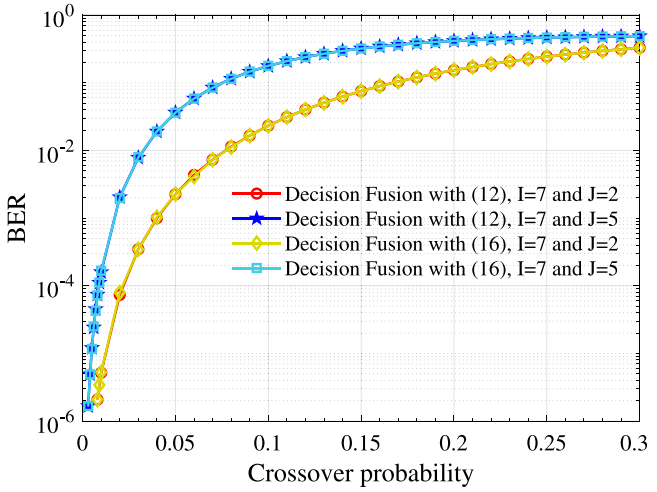

Fig. 22. BER performance comparison of (12) and (16). The number of route is set to be 7, and the relay number is 2 or 5.

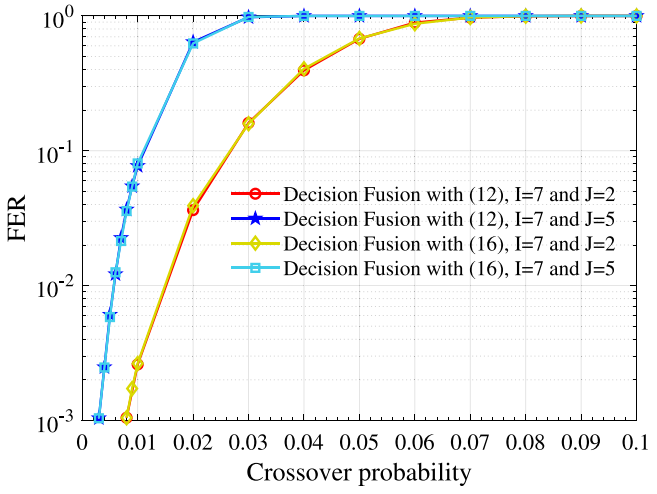

Fig. 23. FER performance comparison of (12) and (16). The number of route is set to be 7, and the relay number is 2 or 5.

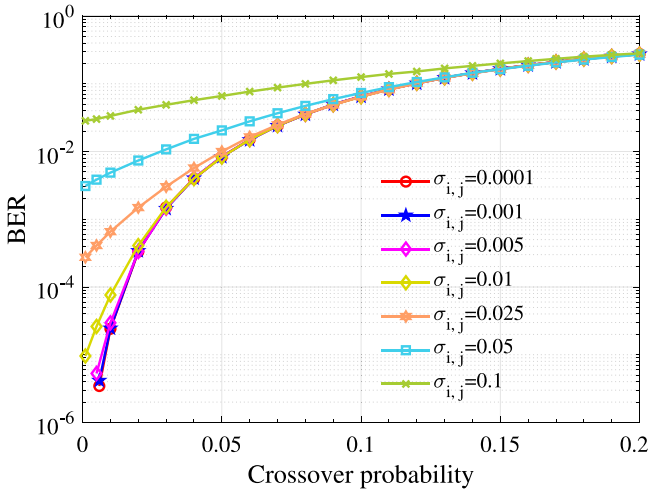

Fig. 24. BER performance of different noise standard deviations under suboptimum decision fusion. The route number is 7 and the relay number is 3.

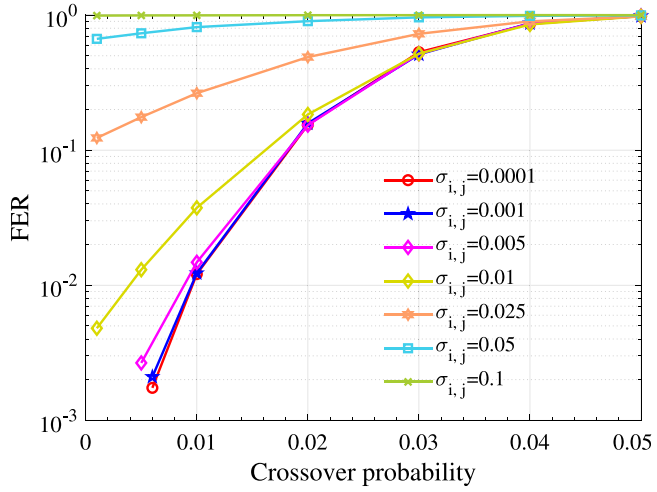

Fig. 25. FER performance of different noise standard deviations under suboptimum decision fusion. The route number is 7 and the relay number is 3.

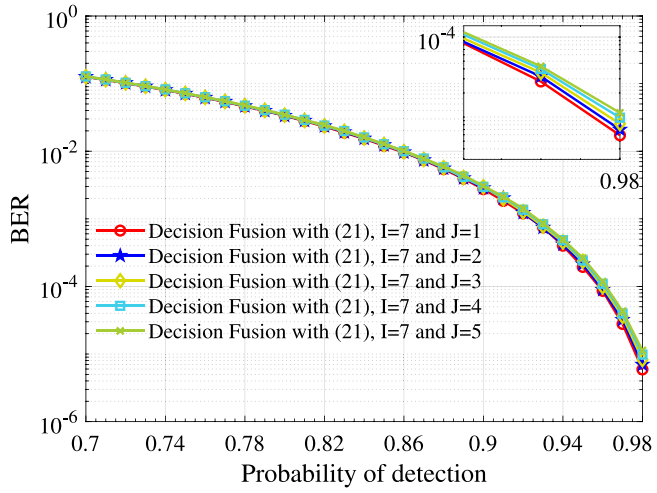

Fig. 26. BER performance of decision fusion with (21). The number of route is set to be 7, and the relay number varies from 1 to 5.

performance is improved as a whole. When the crossover probability is fixed to 0.008, the BER values of 3 and 5 hops are 1.027×10^{-5} and 7.412×10^{-5} respectively under the 7 routes, these values are about half of the previous values.

Secondly, we simulate the suboptimum decision fusion with (16), the results are shown in Figs. 18 to 21. Since the suboptimum decision fusion with (16) is the derivation from the optimal fusion in (12), we want to understand the performance changes of the system while reducing the complexity. Therefore, we choose to compare the two methods when the number of routes is 7 and the number of relays is 2 and 5 respectively. According to the BER and FER in Figs. 22 and 23, we are surprised to find that they are roughly consistent, which shows that while reducing the complexity, the system only depicts a very small loss.

Finally, We study the effect of noise variance on system performance, as shown in Figs. 24 and 25, We can find that when the noise variance is small, it will not have a great impact on the system performance.

8.3. Performance when the relay channel condition is good

In this part, we give the performance with (21) when the relay channel condition is good. We set the crossover probability of each hop

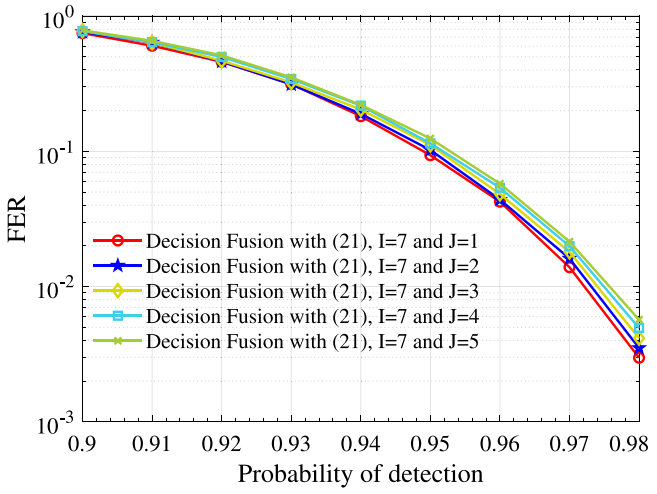

Fig. 27. FER performance of decision fusion with (21). The number of route is set to be 7, and the relay number varies from 1 to 5.

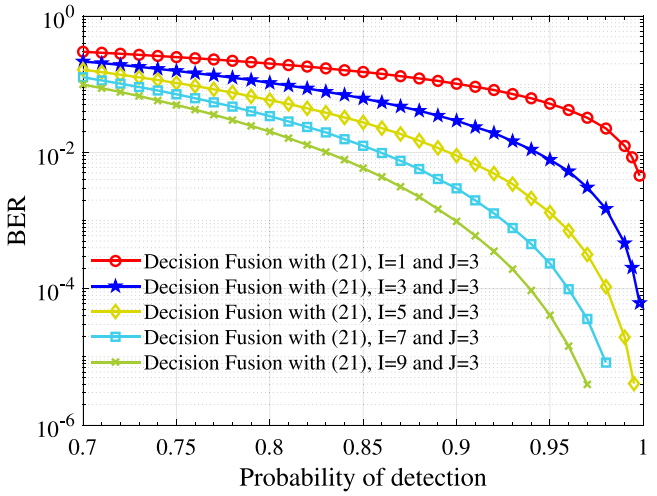

Fig. 28. BER performance of decision fusion with (21). The number of relay is set to be 3, and the route number varies from 1 to 9.

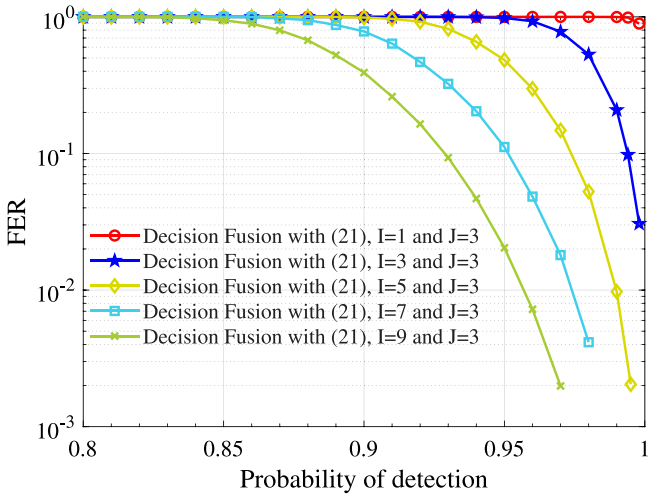

Fig. 29. FER performance of decision fusion with (21). The number of relay is set to be 3, and the route number varies from 1 to 9.

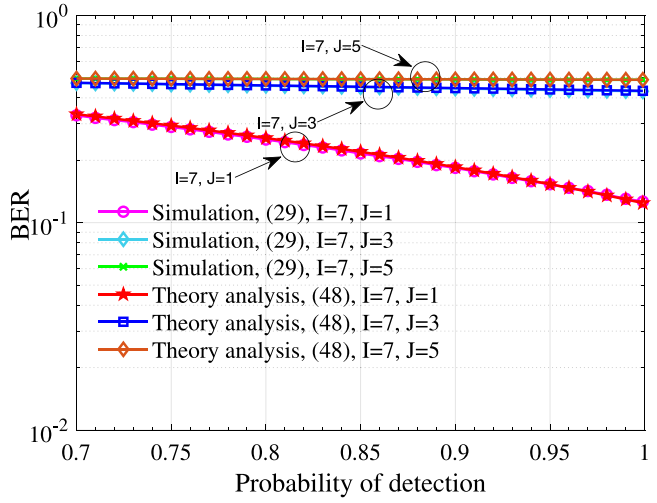

Fig. 30. Simulation result and theory analysis for majority-based fusion decision when the relay channel condition is poor.

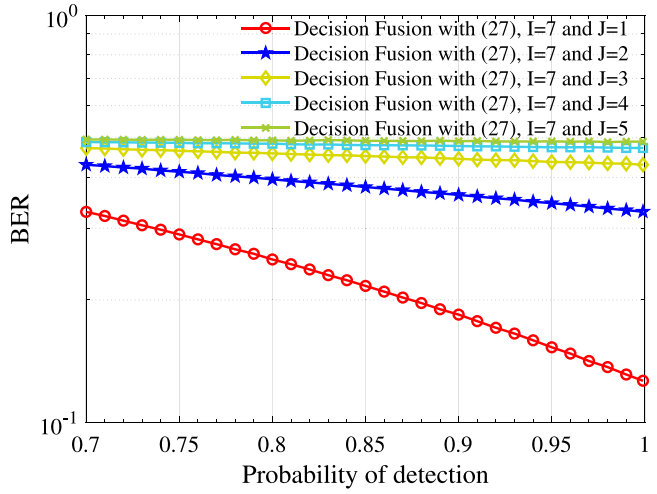

Fig. 31. BER performance of decision fusion with (27). The number of route is set to be 7, and the relay number varies from 1 to 5.

to be 0.001. The false alarm probability P_{fi} and detection probability P_{di} are used to characterize the performance of local sensors. In order not to lose generality, we assume that both the false alarm probability and the detection probability change uniformly. Then we observe the detection performance of the system when the value of P_{di} is changed.

As shown in Figs. 26 and 27, with the increase of the number of relays, the BER and FER do not change significantly. We can see from Fig. 29 that when the number of routes is 3, 5 and 9, the FER values of the system are 7.792×10^{-1}, 1.476×10^{-1} and 1.987×10^{-3} respectively. Here, the detection probability is fixed to 0.97 and the relay number is set to be 3. It can be seen that the routing number has a very significant impact on the performance of the system (see Fig. 28).

8.4. Performance when the relay channel condition is poor

Here, we analyze the performance of decision fusion in (27) and (29) when the relay channel condition is poor. The former decision requires channel status information, while the latter does not. We set the crossover probability of each hop to be 0.3, which means that when there are two hops, the crossover probability of the equivalent BSC channel is 0.42, while when there are six hops, the channel crossover probability is as high as 0.498, close to 0.5, and the channel

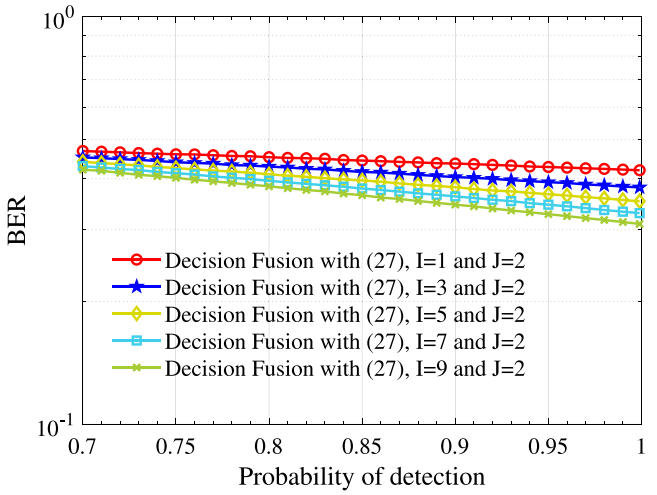

Fig. 32. BER performance of decision fusion with (27). The number of relay is set to be 3, and the route number varies from 1 to 9.

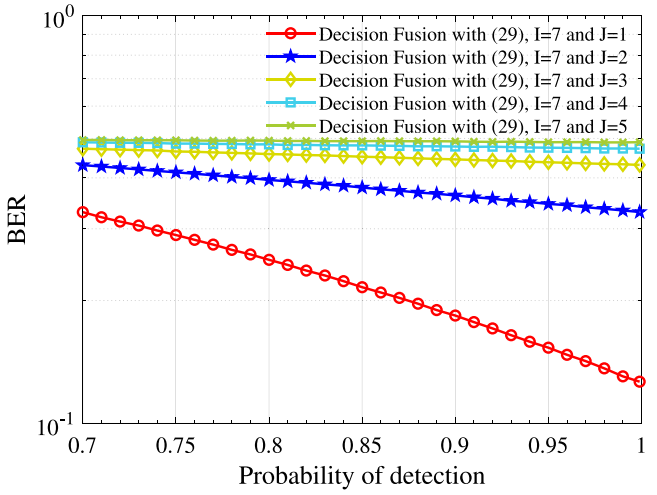

Fig. 33. BER performance of decision fusion with (29). The number of route is set to be 7, and the relay number varies from 1 to 5.

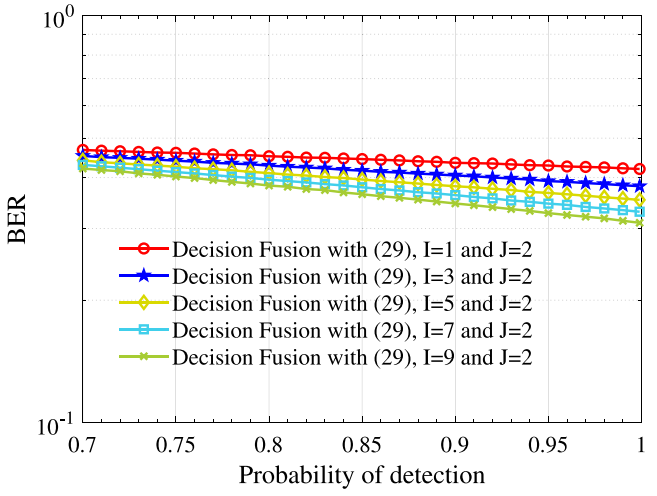

Fig. 34. BER performance of decision fusion with (29). The number of relay is set to be 3, and the route number varies from 1 to 9.

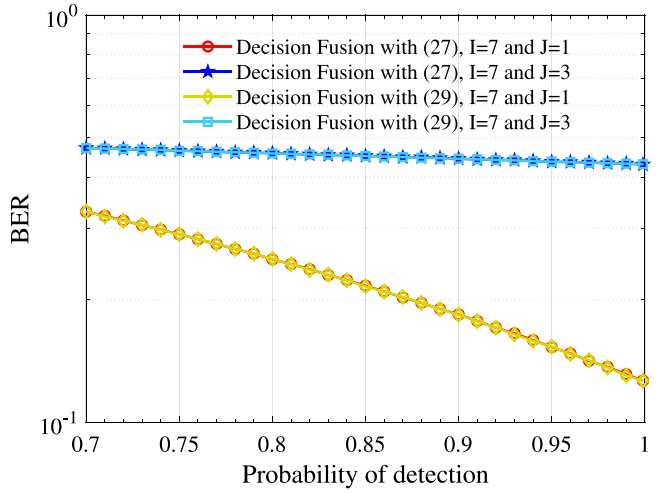

Fig. 35. BER performance comparison of (27) and (29). The number of route is set to be 7, and the relay number is 1 or 3.

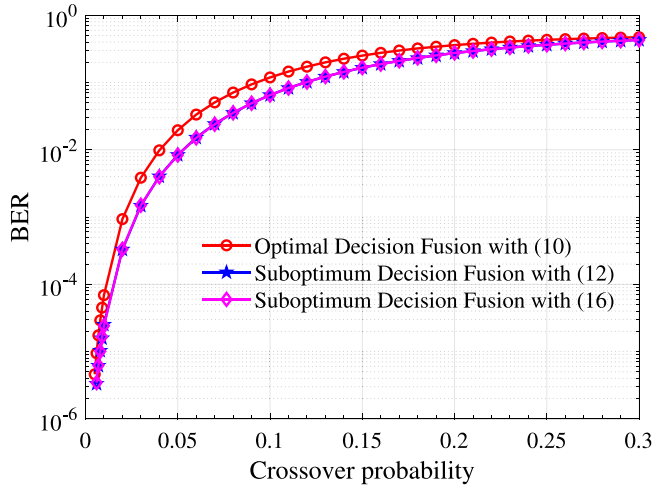

Fig. 36. BER performance comparison of (10), (12) and (16). The number of route is set to be 7, and the relay number is 3.

conditions are poor enough. We observe the performance by changing the detection probability from local channel.

We depict the simulation performance with the theoretical analysis in Fig. 30. We can see that the simulation results are almost in agreement with the theoretical results, which gives strong support to the simulation process.

From Figs. 31 to 34, we simulate the multi hop gain and routing gain of (27) and (29) respectively. Obviously, due to the poor channel conditions, especially when the number of hops is large and the crossover probability of the equivalent BSC channel is close to 0.5, the overall performance of the system is poor, and the bit error rate of both methods is more than 0.1. However, with the increase of detection probability from source to sensor and the number of routes, the performance of the system is improved.

Decision with (27) and (29) are compared in Fig. 35. We can clearly see that although (29) is obtained by (27) using more approximate means, the performance is not greatly affected. When the detection probability is very high, the difference between the BER curve values of the two is about 7×10^{-4}.

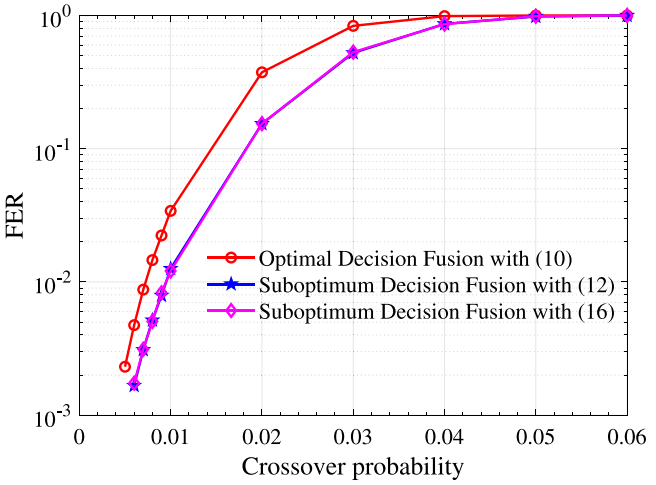

Fig. 37. FER performance comparison of (10), (12) and (16). The number of route is set to be 7, and the relay number is 3.

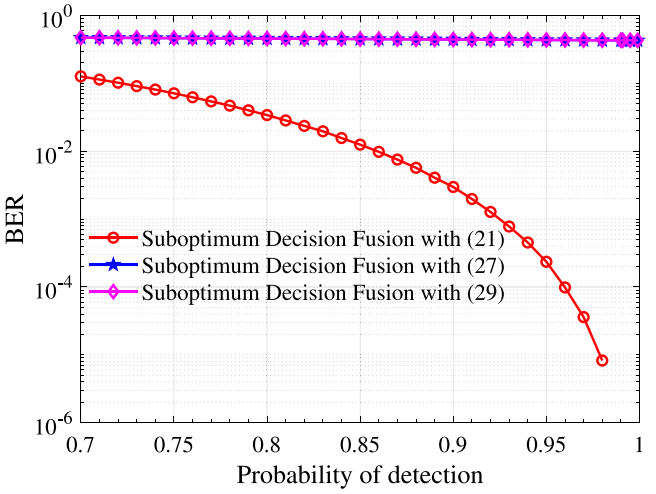

Fig. 38. BER performance comparison of (21), (27) and (29). The number of route is set to be 7, and the relay number is 3.

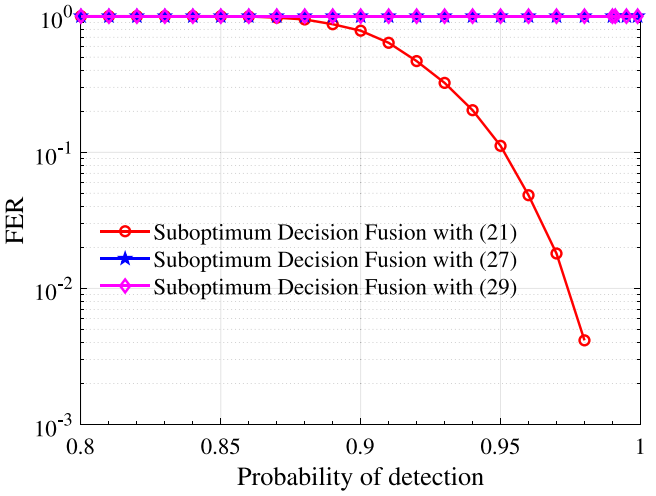

Fig. 39. FER performance comparison of (21), (27) and (29). The number of route is set to be 7, and the relay number is 3.

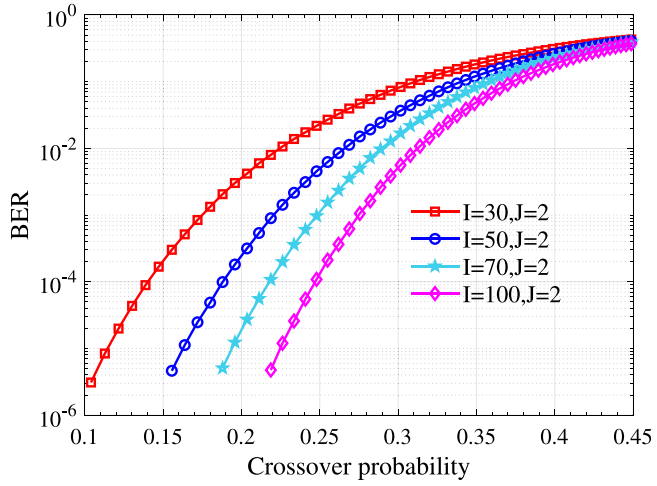

Fig. 40. BER Performance of Joint Decision Fusion. The number of relay is set to be 2, and the route number is 30, 50, 70 and 100.

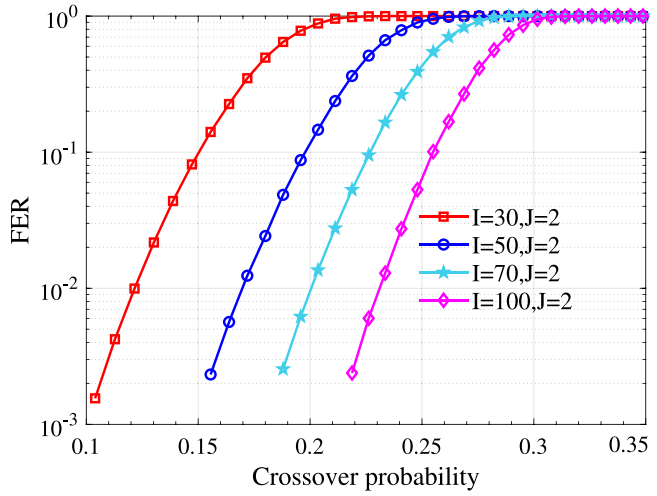

Fig. 41. FER Performance of Joint Decision Fusion. The number of relay is set to be 2, and the route number is 30, 50, 70 and 100.

8.5. Fusion performance comparison

In Figs. 36 to 37, the first two curves represent the BER and FER performance of decision fusion with (10) and (12) under the condition of whether the local channel is ideal or not. The last two curves represent the system performance of decision fusion with (12) and (16) when the local channel is ideal. We can find that when the local sensor channel is ideal, the performance is better than that of the nonideal channel, and the performance of (12) and (16) is roughly consistent.

In Figs. 38 to 39, The red curve is the performance of (21) when the relay channel condition is good, the blue and purple curves are the performance of (27) and (29) when the relay channel condition is poor, and the abscissa represents the detection probability of the local sensor. We can find that when the state of the relay channel condition is good, increasing the performance of the sensor can significantly improve the performance of the whole system.

8.6. Performance for joint decision fusion and CSI estimation

In this part, we use practical joint decision fusion and CSI estimation given in (32), (34) and (35) . According to (36), when $m = 5$, we select 0.1, 0.2, 0.3 and 0.4 as the quantization value. In order to show better

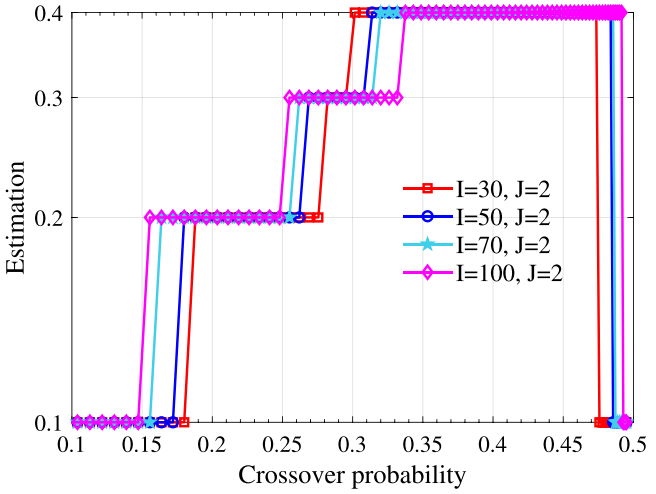

Fig. 42. The Performance of CSI Estimation. The number of relay is set to be 2, and the route number is 30, 50, 70 and 100.

estimation and detection performance, we consider the scenario where more routes are used in the communication process. The relay is set to be 2 hops and the route number is 30, 50, 70 or 100. The crossover probability of each hop is set to be 0.1 to 0.45.

In Figs. 40 to 41, we can see that in 30 sensors, when the crossover probability is around 0.1, the BER is close to 1×10^{-6}, while in 100 sensors, when the crossover probability is around 0.2, the ideal BER and fer curves can be easily obtained. This is also an extension of the previous routing gain.

Let us focus on Fig. 42, which perfectly presents the estimation performance of (32) to (36). On the whole, each graph line can estimate the corresponding crossover probability near the actual crossover probability. However, it can be found in detail that when the number of routes is low, a more accurate estimation can only be obtained near the crossover probability, while when the number of routes is high, the threshold of estimation becomes broader. For 30 routes, an estimated value of 0.2 is obtained when the crossover probability is close to 0.18, while for 100 routes, it is obtained in advance when the crossover probability is 0.155, so that we can see that the estimated performance improves considerably as the number of routes increases. However, when the channel conditions are very poor, the estimation performance is also greatly affected, such as when the crossover probability is close to 0.5.

8.7. Complexity analysis

We compare the implementation complexity of various detection schemes in Table 2. Note that, we have previously assumed that the number of 1 in the local observation is denoted as K_1, and the number of 0 is denoted as K_0 in Section 7. Obviously, the multiplication and division of the approximated formula operation is greatly reduced, making the system simple and easy to implement.

9. Conclusions and future work

Decision fusion for multi-route and multi-hop WSNs over the BSC is developed. An explicit and exact solution for the optimum LLR-based statistic is derived, which however perfect knowledge of the CSI for each BSC and the local sensor performance indices is required at the FC. The simple and robust suboptimum LLR-based fusion rules for two cases are thus developed, wherein less or no a priori information is required. More importantly, the joint decision fusion and CSI estimation is also studied, and the optimal LLR-based scheme is proposed. However, our result show that this optimal joint decision fusion and estimation

Table 2
Comparison of the complexity of different schemes.

Decision fusion scheme	$(\bullet)\pm(\bullet)$	$(\bullet)(\bullet)$ or $(\bullet)/(\bullet)$	$\ln(\bullet)$	CSI	P_{di} and P_{fi}
(10)	$(7+2J)(I-1)$	$(J(J-1)+5)I$	I	yes	yes
(16)	$I(I-1)$	I	0	no	no
(21)	$2K_0+K_1-1$	I	I	no	yes
(29)	$I(I-1)$	I	0	no	no

scheme is computationally practical. In order to simplify the fusion detectors, we give a suboptimum scheme, wherein the continuous CSI is quantized into discrete status. The fusion detection performance at the FC is conducted through simulations.

There are several directions remaining for future research. First, we pay all our attention towards decision fusion without channel coding. The extension to coded case, wherein the local sensor is equipped with an encoder, is worthy of further study. In this case, soft-decision data can be transmitted in the relay node, and much decoding gain is expected to be achieved at the FC. For convenience of analysis, we assume that the local sensors observe independent noisy versions of the source, and the extension to the correlation case is also worthy of further study. Then, the energy consumption is also a challenging problem, and the optimal number of hops minimizing the total energy consumption of decision fusion for multi-route and multi-hop WSNs is also a direction worth studying. Finally, artificial neural network (ANN), which has been quickly developed in recent years, is also a direction worth studying [30–33]. This follows from the fact that a neural network type decoder is available and a large amount of training data can be configured to simulate the channel transitions. In this condition, there is also no need for estimation of the CSI.

CRediT authorship contribution statement

Gaoyuan Zhang: Wrote the paper, Modifying the paper, Literature review and the discussion of the results. **Kai Chen:** Algorithm design, Performed all the simulations under the supervision and guidance of Gaoyuan Zhang, Sravan Kumar Reddyc and Congzheng Han, Wrote the paper, Preparing and analyzing the simulation data under the supervision and guidance of Congzheng Han, Modifying the paper, Literature review and the discussion of the results. **Congfang Ma:** Algorithm design, Performed all the simulations under the supervision and guidance of Gaoyuan Zhang, Sravan Kumar Reddyc and Congzheng Han, Modifying the paper, Literature review and the discussion of the results. **Sravan Kumar Reddy:** Modifying the paper, Literature review and the discussion of the results. **Baofeng Ji:** Modifying the paper, Literature review and the discussion of the results. **Yongen Li:** Preparing and analyzing the simulation data under the supervision and guidance of Congzheng Han, Modifying the paper, Literature review and the discussion of the results. **Congzheng Han:** Modifying the paper, Literature review and the discussion of the results. **Xiaohui Zhang:** Modifying the paper, Literature review and the discussion of the results. **Zhumu Fu:** Modifying the paper, Literature review and the discussion of the results.

Declaration of competing interest

The authors declare that they have no known competing financial interests or personal relationships that could have appeared to influence the work reported in this paper.

Data availability

Data will be made available on request.

Acknowledgments

This research was funded by the National Natural Science Foundation of China grant numbers [61701172 and 41605122], the Key Laboratory of Middle Atmosphere and Global environment Observation grant number [LAGEO-2021-04], the backbone teacher training program of HAUST, the Natural Science Foundation of Henan Province, China grant number [162300410097], and the Scientific and Technological Innovation Team of Colleges and Universities in Henan Province, China grant number [20IRTSTHN018].

Appendix

$$
\begin{aligned}
\Lambda(y_i) &= \log\frac{P(H_1|y_i)}{P(H_0|y_i)} \\
&= \log\frac{P(H_1,x_i=0,y_i)+P(H_1,x_i=1,y_i)}{P(u=0,x_i=0,y_i)+P(u=0,x_i=1,y_i)} \\
&= \log\frac{\begin{array}{l}P(H_1|x_i=0,y_i)P(x_i=0,y_i)+\\ P(H_1|x_i=1,y_i)P(x_i=1,y_i)\end{array}}{\begin{array}{l}P(H_0|x_i=0,y_i)P(x_i=0,y_i)+\\ P(H_0|x_i=1,y_i)P(x_i=1,y_i)\end{array}} \\
&= \log\frac{\begin{array}{l}P(H_1|x_i=0)P(x_i=0|y_i)P(x_i=0)+\\ P(H_1|x_i=1)P(x_i=1|y_i)P(x_i=1)\end{array}}{\begin{array}{l}P(H_0|x_i=0)P(x_i=0|y_i)P(x_i=0)+\\ P(H_0|x_i=1)P(x_i=1|y_i)P(x_i=1)\end{array}} \\
&= \log\frac{\begin{array}{l}P(H_1|x_i=0)P(x_i=0|y_i)+\\ P(H_1|x_i=1)P(x_i=1|y_i)\end{array}}{\begin{array}{l}P(H_0|x_i=0)P(x_i=0|y_i)+\\ P(H_0|x_i=1)P(x_i=1|y_i).\end{array}}
\end{aligned}
\tag{53}
$$

Owing to

$$
\begin{aligned}
&P(H_1|x_i=0)P(x_i=0|y_i) \\
&= \frac{P(x_i=0|H_1)P(H_1)}{P(x_i=0)}\frac{P(y_i|x_i=0)P(x_i=0)}{P(y_i)} \\
&= \frac{P(x_i=0|H_1)P(H_1)P(y_i|x_i=0)}{P(y_i)}.
\end{aligned}
\tag{54}
$$

Similarly, we can get:

$$
\begin{cases}
P(H_1|x_i=1)P(x_i=1|y_i) \\
= \frac{P(x_i=1|H_1)P(H_1)P(y_i|x_i=1)}{P(y_i)} \\
P(H_0|x_i=0)P(x_i=0|y_i) \\
= \frac{P(x_i=0|H_0)P(H_0)P(y_i|x_i=0)}{P(y_i)} \\
P(H_0|x_i=1)P(x_i=1|y_i) \\
= \frac{P(x_i=1|H_0)P(H_0)P(y_i|x_i=1)}{P(y_i)}.
\end{cases}
\tag{55}
$$

Substituting (54) and (55) into $\Lambda\left(y_i\right)$, we have

$$\begin{aligned}\Lambda\left(y_i\right) &= \log \frac{\begin{array}{c}P\left(x=0\left|H_1\right.\right) P\left(H_1\right) P\left(y_i\left|x_i=0\right.\right)+\\ P\left(x_i=1\left|H_1\right.\right) P\left(H_1\right) P\left(y_i\left|x_i=1\right.\right)\end{array}}{\begin{array}{c}P\left(x_i=0\left|H_0\right.\right) P\left(H_0\right) P\left(y_i\left|x_i=0\right.\right)+\\ P\left(x_i=1\left|H_0\right.\right) P\left(H_0\right) P\left(y_i\left|x_i=1\right.\right)\end{array}} \\ &= \log \frac{\begin{array}{c}P\left(x_i=0\left|H_1\right.\right) P\left(y_i\left|x_i=0\right.\right)+\\ P\left(x_i=1\left|H_1\right.\right) P\left(y_i\left|x_i=1\right.\right)\end{array}}{\begin{array}{c}P\left(x_i=0\left|H_0\right.\right) P\left(y_i\left|x_i=0\right.\right)+\\ P\left(x_i=1\left|H_0\right.\right) P\left(y_i\left|x_i=1\right.\right)\end{array}} \\ &= \log \frac{P_{di} P\left(y_i\left|x_i=1\right.\right)+\left(1-P_{di}\right) P\left(y_i\left|x_i=0\right.\right)}{P_{fi} P\left(y_i\left|x_i=1\right.\right)+\left(1-P_{fi}\right) P\left(y_i\left|x_i=0\right.\right)}.\end{aligned} \tag{56}$$

References

[1] L. Xu, X. Zhou, X. Li, R.H. Jhaveri, T.R. Gadekallu, Y. Ding, Mobile collaborative secrecy performance prediction for artificial IoT networks, IEEE Trans. Ind. Inf. 18 (8) (2022) 5403–5411, http://dx.doi.org/10.1109/TII.2021.3128506.

[2] H. Wang, X. Li, R.H. Jhaveri, T.R. Gadekallu, M. Zhu, T.A. Ahanger, S.A. Khowaja, Sparse Bayesian learning based channel estimation in FBMC/OQAM industrial IoT networks, Comput. Commun. 176 (2021) 40–45, http://dx.doi.org/10.1016/j.comcom.2021.05.020.

[3] X. Li, X. Gao, Y. Liu, G. Huang, M. Zeng, D. Qiao, Overlay cognitive radio-assisted NOMA intelligent transportation systems with imperfect SIC and CEEs, Chinese J. Electron. (2022).

[4] X. Huan, K.S. Kim, S. Lee, E.G. Lim, A. Marshall, Improving multi-hop time synchronization performance in wireless sensor networks based on packet-relaying gateways with per-hop delay compensation, IEEE Trans. Commun. 69 (9) (2021) 6093–6105, http://dx.doi.org/10.1109/TCOMM.2021.3092038.

[5] Y. Zhang, C. Jiang, B. Yue, J. Wan, M. Guizani, Information fusion for edge intelligence: A survey, Inf. Fusion 81 (2022) 171–186, http://dx.doi.org/10.1016/j.inffus.2021.11.018.

[6] X. Liu, X. Liu, Asymptotically optimal link bit error probability for distributed detection in wireless sensor networks, Comput. Commun. 176 (2021) 155–162, http://dx.doi.org/10.1016/j.comcom.2021.05.022.

[7] A. Chawla, P.S. Kumar, S. Srivastava, A.K. Jagannatham, Centralized and distributed millimeter wave massive MIMO-based data fusion with perfect and Bayesian learning (BL)-based imperfect CSI, IEEE Trans. Commun. 70 (3) (2022) 1777–1791, http://dx.doi.org/10.1109/TCOMM.2022.3141411.

[8] P.V. Ivanovich, L.V. Dong, Optimal fusion rule for distributed detection with channel errors taking into account sensors' unreliability probability when protecting coastlines, Int. J. Sensor Netw. 38 (2) (2022) 71–84, http://dx.doi.org/10.1504/IJSNET.2022.121157.

[9] N. Sriranga, K.G. Nagananda, R.S. Blum, A. Saucan, P.K. Varshney, Energy-efficient decision fusion for distributed detection in wireless sensor networks, in: 2018 21st International Conference on Information Fusion, FUSION, 2018, pp. 1541–1547, http://dx.doi.org/10.23919/ICIF.2018.8454976.

[10] Y. Abdi, T. Ristaniemi, The max-product algorithm viewed as linear data-fusion: A distributed detection scenario, IEEE Trans. Wireless Commun. 19 (11) (2020) 7585–7597, http://dx.doi.org/10.1109/TWC.2020.3012910.

[11] Y. Lin, B. Chen, P.K. Varshney, Decision fusion rules in multi-hop wireless sensor networks, IEEE Trans. Aerosp. Electron. Syst. 41 (2) (2005) 475–488, http://dx.doi.org/10.1109/TAES.2005.1468742.

[12] S. Karimi-Bidhendi, J. Guo, H. Jafarkhani, Energy-efficient deployment in static and mobile heterogeneous multi-hop wireless sensor networks, IEEE Trans. Wireless Commun. 21 (7) (2022) 4973–4988, http://dx.doi.org/10.1109/TWC.2021.3135385.

[13] Z. Lin, H.-C. Keh, R. Wu, D.S. Roy, Joint data collection and fusion using mobile sink in heterogeneous wireless sensor networks, IEEE Sens. J. 21 (2) (2021) 2364–2376, http://dx.doi.org/10.1109/JSEN.2020.3019372.

[14] C. Li, G. Li, P.K. Varshney, Distributed detection of sparse signals with censoring sensors in clustered sensor networks, Inf. Fusion 83 (2022) 1–18, http://dx.doi.org/10.1016/j.inffus.2022.03.002.

[15] F.H. El-Fouly, R.A. Ramadan, E3AF: energy efficient environment-aware fusion based reliable routing in wireless sensor networks, IEEE Access 8 (2020) 112145–112159, http://dx.doi.org/10.1109/ACCESS.2020.3003155.

[16] V.K. Akram, Distributed detection of minimum cuts in wireless multi-hop networks, IEEE Trans. Comput. 71 (4) (2022) 919–932, http://dx.doi.org/10.1109/TC.2021.3065527.

[17] Y.-R. Tsai, L.-C. Lin, Sequential fusion for distributed detection over BSC channels in an inhomogeneous sensing environment, IEEE Signal Process. Lett. 17 (1) (2010) 99–102, http://dx.doi.org/10.1109/LSP.2009.2034552.

[18] G. Zhang, C. Shi, C. Han, X. Li, D. Wang, K. Rabie, R. Kharel, Implementation-friendly and energy-efficient symbol-by-symbol detection scheme for IEEE 802.15. 4 O-QPSK receivers, IEEE Access 8 (2020) 158402–158415, http://dx.doi.org/10.1109/ACCESS.2020.3020183.

[19] C. Shi, G. Zhang, H. Li, C. Han, J. Tang, H. Wen, L. Wang, D. Wang, Reduced-complexity multiple-symbol detection of O-QPSK signals in smart metering utility networks, Electronics 9 (12) (2020) 1–25, http://dx.doi.org/10.3390/electronics9122049.

[20] G. Zhang, H. Wen, L. Wang, L. Song, J. Tang, R. Liao, Simple and robust near-optimal single differential detection scheme for IEEE 802.15. 4 BPSK receivers, IET Commun. 13 (2) (2019) 186–197, http://dx.doi.org/10.1049/iet-com.2018.5047.

[21] G. Zhang, H. Wen, L. Wang, X. Zeng, J. Tang, R. Liao, L. Song, Multiple symbol differential detection scheme for IEEE 802.15. 4 BPSK receivers, IEICE Trans. Fundam. Electron. Commun. Comput. Sci. 101 (11) (2018) 1975–1979, http://dx.doi.org/10.1587/transfun.E101.A.1975.

[22] G. Zhang, H. Wen, L. Wang, P. Xie, L. Song, J. Tang, R. Liao, Simple adaptive single differential coherence detection of BPSK signals in IEEE 802.15. 4 wireless sensor networks, Sensors 18 (1) (2017) 52, http://dx.doi.org/10.3390/s18010052.

[23] G. Zhang, C. Han, B. Ji, C. Shi, P. Xie, L. Yang, A new multiple-symbol differential detection strategy for error-floor elimination of IEEE 802.15. 4 BPSK receivers impaired by carrier frequency offset, Wirel. Commun. Mob. Comput. 2019 (3) (2019) 1–26, http://dx.doi.org/10.1155/2019/5409612.

[24] G. Zhang, D. Wang, L. Song, H. Wu, P. Xie, B. Ji, H. Wen, Simple non-coherent detection scheme for IEEE 802.15. 4 BPSK receivers, Electron. Lett. 53 (9) (2017) 628–629, http://dx.doi.org/10.1049/el.2017.0196.

[25] G. Zhang, H. Li, C. Han, C. Shi, H. Wen, D. Wang, Multiple-symbol detection scheme for IEEE 802.15. 4c MPSK receivers over slow Rayleigh fading channels, Secur. Commun. Netw. 2021 (2021) 19, http://dx.doi.org/10.1155/2021/6641192.

[26] G. Zhang, H. Li, C. Han, C. Shi, X. Zhang, Multiple symbol detection for convolutional coded O-QPSK signals in smart metering utility networks without channel state information, Phys. Commun. 49 (2021) 101490, http://dx.doi.org/10.1016/j.phycom.2021.101490.

[27] G. Zhang, H. Wen, J. Pu, J. Tang, Build-in wiretap channel I with feedback and LDPC codes by soft decision decoding, IET Commun. 11 (11) (2017) 1808–1814, http://dx.doi.org/10.1049/iet-com.2016.0880.

[28] W. Ryan, S. Lin, Channel Codes: Classical and Modern, Cambridge University Press, New York, USA, 2009.

[29] T. Richardson, R. Urbanke, Modern Coding Theory, Cambridge University Press, New York, USA, 2008.

[30] J. Hagenauer, E. Offer, L. Papke, Iterative decoding of binary block and convolutional codes, IEEE Trans. Inform. Theory 42 (2) (1996) 429–445, http://dx.doi.org/10.1109/18.485714.

[31] S. Zheng, S. Chen, X. Yang, Deepreceiver: a deep learning-based intelligent receiver for wireless communications in the physical layer, IEEE Trans. Cogn. Commun. Netw. 7 (1) (2021) 5–20, http://dx.doi.org/10.1109/TCCN.2020.3018736.

[32] X. Chen, H. Li, J. Qu, A. Razi, Boosting belief propagation for LDPC codes with deep convolutional neural network predictors, in: 2021 IEEE 18th Annual Consumer Communications & Networking Conference, CCNC, IEEE, 2021, pp. 1–6, http://dx.doi.org/10.1109/CCNC49032.2021.9369460.

[33] I. Be'Ery, N. Raviv, T. Raviv, Y. Be'Ery, Active deep decoding of linear codes, IEEE Trans. Commun. 68 (2) (2020) 728–736, http://dx.doi.org/10.1109/TCOMM.2019.2955724.